

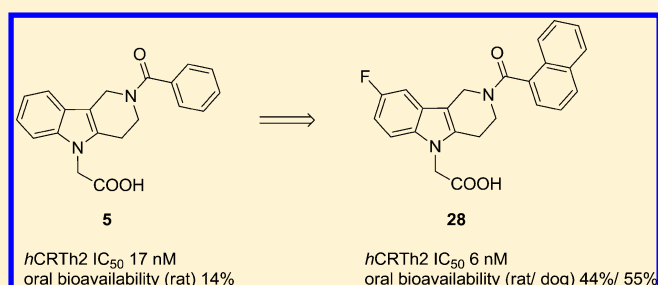
Identification of 2-(2-(1-Naphthoyl)-8-fluoro-3,4-dihydro-1H-pyrido[4,3-b]indol-5(2H)-yl)acetic Acid (Setipiprant/ACT-129968), a Potent, Selective, and Orally Bioavailable Chemoattractant Receptor-Homologous Molecule Expressed on Th2 Cells (CRTh2) Antagonist

Heinz Fretz,* Anja Valdenaire, Julien Pothier, Kurt Hilpert, Carmela Gnerre, Oliver Peter, Xavier Leroy, and Markus A. Riederer

Drug Discovery Unit, Actelion Pharmaceuticals Ltd., Gewerbestrasse 16, CH-4123 Allschwil, Switzerland

Supporting Information

ABSTRACT: Herein we describe the discovery of the novel CRTh2 antagonist 2-(2-(1-naphthoyl)-8-fluoro-3,4-dihydro-1H-pyrido[4,3-b]indol-5(2H)-yl)acetic acid **28** (setipiprant/ACT-129968), a clinical development candidate for the treatment of asthma and seasonal allergic rhinitis. A lead optimization program was started based on the discovery of the recently disclosed CRTh2 antagonist 2-(2-(benzoyl)-3,4-dihydro-1H-pyrido[4,3-b]indol-5(2H)-yl)acetic acid **5**. An already favorable and druglike profile could be assessed for lead compound **5**. Therefore, the lead optimization program mainly focused on the improvement in potency and oral bioavailability. Data of newly synthesized analogs were collected from in vitro pharmacological, physicochemical, in vitro ADME, and in vivo pharmacokinetic studies in the rat and the dog. The data were then analyzed using a traffic light selection tool as a visualization device in order to evaluate and prioritize candidates displaying a balanced overall profile. This data-driven process and the excellent results of the PK study in the rat ($F = 44\%$) and the dog ($F = 55\%$) facilitated the identification of **28** as a potent ($IC_{50} = 6$ nM), selective, and orally available CRTh2 antagonist.



INTRODUCTION

Allergic disorders, such as asthma, allergic rhinitis, and atopic dermatitis, represent an increasing global health problem,¹ and despite clear advances in therapy, the disease of many patients is not adequately controlled. There is a clear medical need for additional, efficacious, safe, and orally active drugs for allergic disorders.^{2,3}

Prostaglandin D₂ (PGD₂) **1** (Chart 1) is a lipid mediator synthesized from arachidonic acid via the cyclooxygenase (COX) and prostaglandin D₂ synthase (PGDS) pathway. PGD₂ is produced in the brain where it is involved in regulating central nervous functions such as sleep and pain perception. In the periphery, mast cells are the initial source of PGD₂. These tissue-resident cells are presenting allergen-specific IgE-antibodies on their surface. Upon encounter with allergens, clustering of IgE antibodies induces an intracellular signaling cascade, leading to the generation of PGD₂.^{4,5} In patients suffering from allergic asthma, PGD₂ and its metabolites are increased in the lung, plasma, and urine.^{6,7}

Chemoattractant receptor-homologous molecule expressed on T helper 2 cells (CRTh2) is a G-protein-coupled receptor (GPCR) for PGD₂.⁸ The expression of CRTh2 is limited to eosinophils, basophils, Th2 cells, and innate lymphoid cells.^{8,9} Activation of CRTh2 induces a marked increase in mobility,

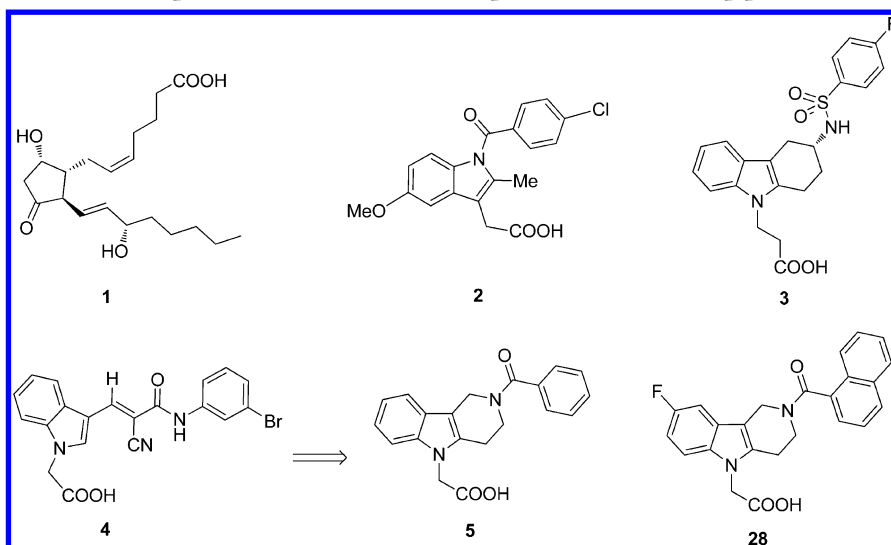
degranulation, and expression of adhesion molecules in eosinophils and basophils.^{8,10,11} In addition, upon activation of CRTh2 by PGD₂, Th2 cells can secrete Th2-specific cytokines, such as interleukin (IL) 4, IL-5, and IL-13,^{10,12} responsible for enhancing eosinophilia, tissue remodeling, and airway hypersensitivity.^{13,14}

Mice deficient in CRTh2 have been described to be resistant to experimentally induced allergic asthma, suggesting that CRTh2 might play a central role in the pathogenesis of allergic diseases.¹⁵ Therefore, low molecular weight antagonists of CRTh2 were expected to counteract pathophysiological effects of PGD₂ and thus to display controlling effects on allergic inflammation.¹⁶

The first non-prostanoid CRTh2 modulators have already been described a decade ago. For example, **2** (indomethacin), a nonsteroidal anti-inflammatory drug (NSAID) acting as a nonselective inhibitor of COX-1 and COX-2 enzymes that participate in prostaglandin synthesis from arachidonic acid,¹⁷ was discovered to act as a partial agonist on CRTh2,¹⁸ whereas **3** (ramatroban, BAY u3405), a human thromboxane A₂ (TXA₂) receptor (hTP_2) antagonist with clinical efficacy in

Received: January 25, 2013

Chart 1. Structure of Endogenous CRTh2 Agonist PGD₂ (1), Partial Agonist Indomethacin (2), Antagonist Ramatroban (3), Primary Screening Hit 4, Lead Compound 5, and Clinical Development Candidate Setipiprant/ACT-129968 (28)



asthma and allergic rhinitis,^{19–21} was the first small molecule CRTh2 antagonist disclosed, displaying inhibitory activity of in vitro PGD₂-induced eosinophil migration.²² Meanwhile the discovery of numerous CRTh2 antagonists have been described and are currently in early proof-of-concept clinical studies for treating the signs and symptoms of both asthma and allergic rhinitis.²³

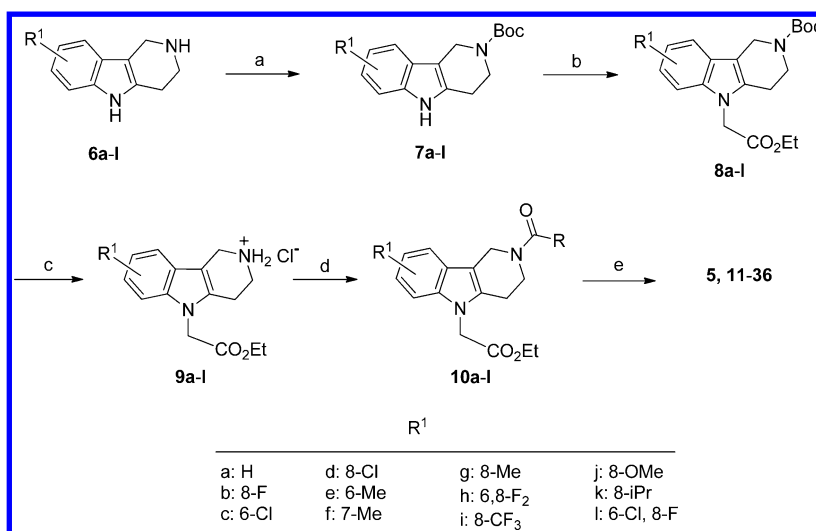
Herein, the lead optimization of a novel chemotype series providing potent, selective, and orally available CRTh2 antagonists is described. Initially identified as a singleton out of 80 000 compounds from a GPCR focused library, high-throughput screening hit 4 was confirmed as a true hit belonging to a cluster of close analogues that displayed a clear structure–activity relationship (SAR).²⁴ Attempts to eliminate potentially unwanted structural features led to the successful design of novel CRTh2 antagonist scaffolds. From this work, 2-(2-benzoyl-3,4-dihydro-1*H*-pyrido[4,3-*b*]indol-5(2*H*)-yl)acetic acid 5 evolved as a novel druglike lead compound devoid of any structural alerts.²⁴ The goal of the subsequent lead optimization program was mainly focused on the improvement in potency and oral bioavailability. In vitro pharmacological and physicochemical and in vitro absorption, distribution, and metabolism (ADME) properties of the novel CRTh2 antagonists as well as in vivo pharmacokinetic studies in the rat and the dog will be presented. Furthermore, the data driven process will be discussed which led to the decision to select 2-(2-(1-naphthoyl)-8-fluoro-3,4-dihydro-1*H*-pyrido[4,3-*b*]indol-5(2*H*)-yl)acetic acid 28 (setipiprant/ACT-129968), as a clinical development candidate for the treatment of asthma and seasonal allergic rhinitis.

RESULTS AND DISCUSSION

Biological Assays. Following our screening cascade, a competitive radioligand displacement assay was used as a biological in vitro test system to establish the structure–activity relationship (SAR) for all synthesized potential human (*h*) CRTh2 modulators of this novel 2-(3,4-dihydro-1*H*-pyrido[4,3-*b*]indol-5(2*H*)-yl)acetic acid series. The receptor binding assay was performed with human embryonic kidney (HEK-293) cells stably expressing *h*CRTh2 using [³H]PGD₂ (2.5 nM, 170 Ci/mmol) as radioligand. Quantification of intracellular Ca²⁺

liberation (Ca²⁺ flux, FLIPR) or cyclic (c) AMP were used to give evidence that the compounds are truly antagonizing *h*CRTh2 mediated downstream signaling. The results from both assays are reported as IC₅₀ values. Cross-selectivity with other prostanoid receptors was addressed by counterscreening the compounds against the human PGD₂ receptor *h*DP₁, against the human prostaglandin E₂ (PGE₂) receptor subtypes *h*EP₁, *h*EP₂, *h*EP₃, and *h*EP₄, and against the human thromboxane A₂ receptor *h*TP₂. Cell lines stably expressing recombinant human receptors were used: Chinese hamster ovary (CHO) and HEK-293 cells for *h*EP₁ and *h*EP₃ receptors, respectively, membranes from HEK-293 cells containing *h*EP₂ or *h*EP₄ receptors, and HEK-293 cells stably expressing human *h*TP₂ receptors. Reported are IC₅₀ values defined as half-maximal inhibition of receptor stimulation using an agonist concentration previously determined to trigger 80% of maximal response. Selectivity of the antagonists toward the *h*DP₁ receptor was determined by using a competitive receptor binding assay with CHO cells stably expressing high levels of recombinant *h*DP₁ receptor, employing [³H]PGD₂ as ligand.²⁵ Reported are the respective IC₅₀ values and the selectivity factor (*f*_{sel}) between *h*DP₁ and *h*CRTh2 which is expressed as the IC₅₀(*h*DP₁)/IC₅₀(*h*CRTh2) ratio. Furthermore, the potential of 2-(3,4-dihydro-1*H*-pyrido[4,3-*b*]indol-5(2*H*)-yl)acetic acid analogues to inhibit COX enzymes was addressed because of the structural similarity with NSAID 2, a nonselective inhibitor of COX enzymes.¹⁷ COX inhibition was assessed using a commercially available ovine COX-1 assay kit from Cayman Chemicals (catalog no. 760111). The compounds were tested in duplicate at 10 μM final concentration according to the protocol provided by the kit manufacturer.

Potent antagonists with binding IC₅₀ < 100 nM were further verified in a competitive radioligand displacement assay in the presence of 0.5% human serum albumin (HSA) in order to identify those antagonists that retained potency under conditions where binding to plasma proteins occurs. The positives were subsequently tested in the eosinophil shape change (*h*ESC) assay.^{26,27} In brief, human eosinophils were isolated from whole blood of healthy volunteers and were subsequently stimulated with 15 nM PGD₂ in the presence of

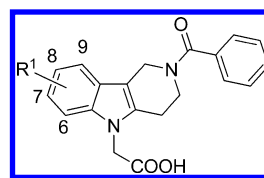
Scheme 1. General Synthetic Scheme for the Preparation of 2-(3,4-Dihydro-1H-pyrido[4,3-*b*]indol-5(2H)-yl)acetic Acid Derivatives 5 and 11–36^a

^aReagents: (a) Boc₂O, DIPEA or Et₃N, DCM or THF, room temperature, 53–100%; (b) BrCH₂CO₂Et, Cs₂CO₃, DMF, 80 °C or acetone, room temperature, 41–88% yield; (c) 4 N HCl in 1,4-dioxane, DCM, room temperature, 16–99% yield; (d) R-COCl, DIPEA, DCM, 0 °C to room temperature, 28–98% yield; (e) 0.2 N aqueous NaOH, THF, room temperature, 18–93% yield.

50% human plasma at 37 °C for 5 min. Stimulation was stopped by adding fixation solution, and increase in light scattering reflecting changes in cell shape was measured by flow cytometry. A dose dependent inhibition of this shape change could be demonstrated with potent antagonists by preincubating the cells with increasing concentrations of the respective antagonist for 10 min prior to stimulation with PGD₂.

Chemistry. About 200 novel 2-(3,4-dihydro-1H-pyrido[4,3-*b*]indol-5(2H)-yl)acetic acid analogues were synthesized in four and five steps as depicted in Scheme 1,²⁸ starting with 2,3,4,5-tetrahydro-1H-pyrido[4,3-*b*]indole analogues 6a–l, all available from commercial sources or synthetically accessible following well established procedures. Classical *N*-Boc-protection was followed by an alkylation step of 7a–l with ethyl bromoacetate in the presence of potassium carbonate in DMF at 80 °C or in acetone at room temperature. Removal of the Boc group in 8a–l using 4 N HCl in 1,4-dioxane gave the corresponding hydrochloride salts 9a–l, which were subsequently reacted with the respective acid chloride R-COCl in DCM at 0 °C in the presence of DIPEA as a base to provide amides 10a–l. Saponification of the ethyl ester with 0.2 M aqueous NaOH solution in THF and preparative reverse-phase LC–MS purification provided 2-(3,4-dihydro-1H-pyrido[4,3-*b*]indol-5(2H)-yl)acetic acid derivatives 5 and 11–36 with >95% purity in 18–93% yield.

SAR Studies. An initial SAR was established with 2-(3,4-dihydro-1H-pyrido[4,3-*b*]indol-5(2H)-yl)acetic acid analogues 11–20 (Table 1). The focus of this set of compounds was directed toward the tolerability of a substituent R¹ attached to the indole unit. As illustrated with 12, 15, 16, and 18, compounds were obtained that were by a factor of 2–3 slightly more potent in the radioligand binding assay than lead compound 5, displaying IC₅₀ values of 5, 11, 7, and 9 nM if R¹ at C(8) represented chlorine, methyl, fluorine, and trifluoromethyl, respectively. Methoxy or isopropyl at C(8) seemed to be less favorable (IC₅₀ of 62 and 42 nM) as illustrated with 19 and 20 (Table 1). Generally, up to 10-fold less potent compounds were obtained if R¹ represented

Table 1. Initial SAR Study Exploring R¹ at the Indole Moiety^a

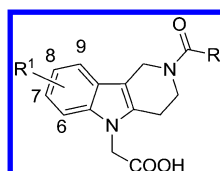
compd	R ¹	<i>h</i> CRTh2 IC ₅₀ [nM] ^b
5	H	17
11	6-Cl	820
12	8-Cl	5
13	6-Me	107
14	7-Me	1590
15	8-Me	11
16	8-F	7
17	6,8-F ₂	35
18	8-CF ₃	9
19	8-MeO	62
20	8- <i>i</i> -Pr	42

^aListed are the IC₅₀ values of the *h*CRTh2 receptor radioligand binding in buffer. ^bThe data represent the means from at least four independent experiments.

chlorine or methyl connected to C(6) or if R¹ was methyl-attached to C(7), as exemplified with 11, 13, or 14, respectively. Combining two fluorine atoms in the same molecule, one connected to the more favorable C(8) position and a second attached to the suboptimal C(6) position, resulted in a more than 5-fold drop in binding affinity as demonstrated with 17. The results of the SAR study exploring R¹ at the indole moiety were in accordance with the data disclosed for the (*E*)-2-cyano-3-(1H-indol-3-yl)acrylamide hit series.²⁴

In another subset of analogues, preferred R¹ residues were combined with various R groups. One-third of those compounds displayed a potent interaction with *h*CRTh2, inhibiting [³H]PGD₂ binding in a competitive manner with

Table 2. SAR Study Exploring R and R¹, with IC₅₀ Binding Data for hCRTh2 of Selected Compounds in Comparison with Lead Compound 5, Measured in the Presence and Absence of Human Serum Albumin (HSA) in the Assay Buffer^a



compd	R ¹	R	hCRTh2 Receptor interaction						Prostanoid receptor interaction			
			Binding in			Ca ²⁺ flux	cAMP	hESC	hDP ₁	f _{sel} ^c	hEP ₂	hEP ₄
			buffer IC ₅₀ [nM]	HSA IC ₅₀ [nM]	f _{HSA} ^b	IC ₅₀ [nM]	IC ₅₀ [nM]	IC ₅₀ [nM]	Binding IC ₅₀ [nM]		β-arrestin IC ₅₀ [nM]	β-arrestin IC ₅₀ [nM]
5	H		17	15	1	170	190	110	>10000	>580	>10000	>10000
18	8-CF ₃		9	60	6	50	160	130	>10000	>1100	>10000	>10000
21	H		70	nd	nd	200	nd	nd	nd	nd	nd	nd
22	8-F		4	12	3	40	70	34	>10000	>2500	>10000	>10000
23	H		10	30	3	70	40	50	>10000	>1000	>10000	>10000
24	8-F		9	60	7	40	95	60	>10000	>1100	>10000	>10000
25	6-Cl, 8-F		190	180	1	1280	nd	nd	4100	22	>10000	>10000
26	H		9	420	47	30	140	1120	780	87	6600	>10000
27	8-Cl		4	65	16	30	110	100	690	230	7400	>10000
28	8-F		6	340	57	30	80	235	1290	215	2600	>10000
29	8-Me		5	190	38	60	nd	340	2700	540	>10000	>10000
30	8-CF ₃		11	70	6	20	380	180	2200	200	>10000	>10000
31	6-Cl, 8-F		70	530	7	660	nd	nd	310	4.1	2700	>10000
32	8-F		4	180	45	70	160	275	>10000	>2500	>10000	>10000
33	8-F		5	35	7	15	40	50	>10000	>2000	>10000	>10000
34	8-F		10	30	3	65	160	210	>10000	>1000	9500	>10000
35	H		4	7	2	190	320	240	780	195	6400	>10000
36	6-Cl		23	90	4	2600	nd	nd	120	5.2	>10000	>10000

^aIC₅₀ values are given for the effects in the cell based Ca²⁺ flux assay, the cAMP homogeneous time resolved fluorescence (HTRF) assay, and the human eosinophil shape change assay. Data are given to demonstrate selectivity against prostanoid receptors hDP₁, hEP₁₋₄ and hTP₂. The IC₅₀ values represent the mean from at least three independent experiments if not stated otherwise. ^bHuman serum albumin shift factor $f_{HSA} = IC_{50}(HSA)/IC_{50}(buffer)$. ^cSelectivity factor $f_{sel} = IC_{50}(hDP1)/IC_{50}(hCRTh2)$.

Table 3. Physicochemical Properties and Ligand Efficiency of Selected Antagonists in Comparison with Lead Compound 5

compd	MW (Da)	LE ^a	cLogP	log <i>D</i> _{7,4}	solubility (μg/mL)		
					water (pH) ^b	buffer, pH 4	buffer, pH 7
5	334.37	0.43	2.09	-1.2	64 (4.3)	515	810
22	358.39	0.46	2.0	0.2	50 (3.9)	80	930
23	368.82	0.42	2.7	-0.5	110 (3.8)	180	815
24	386.81	0.42	2.8	-0.3	25 (4.9)	140	1000
26	384.43	0.38	3.3	0.2	335 (nd)	90	830
28	402.42	0.37	3.3	0.1	50 (4.3)	90	880
32	416.45	0.37	3.1	0.2	28 (5.7)	21	560
33	405.43	0.38	2.0	-0.3	45 (3.8)	115	800
35	438.53	0.35	4.4	1.8	2 (4.3)	1	30

^aLigand efficiency (LE): relative free binding energy in kcal/mol per non-H atom, calculated from IC₅₀ values. ^bpH of the final aqueous solution.

IC₅₀ ≤ 15 nM. A representative selection is listed in Table 2 for a continuing discussion of the SAR. From this list it became evident that hydrophobic R groups were crucial for potent *h*CRTh2 binding, for example, monocyclic five- and six-membered aromatic rings as represented by thiophene and phenyl, directly attached to the carbonyl group, as well as fused aromatic ring systems as illustrated with naphthalene or the nitrogen-containing nonbasic indole, connected either directly or via a methylene or an ethylene bridge to the carbonyl group. The most potent antagonist, 35, was obtained if R represented a biphenyl moiety. Compared to 5, a significant drop in potency was observed if R represents an alkyl group, for example, methyl (IC₅₀ = 1.6 μM) or pentyl (IC₅₀ = 0.2 μM).²⁴ Furthermore, a 5-fold drop in potency was noticed for the respective cyclohexyl analogue 21 (IC₅₀ = 70 nM), consolidating the importance of an aromatic ring system at this site of the molecule. In Table 1, the previously discussed beneficial contributions of fluorine, chlorine, methyl, or trifluoromethyl at C(8) could be strengthened with additional examples listed in Table 2. Also the less favorable effect of C(6) substitution was further established with 25, 31, and 36. These examples displayed an approximately 20-, 12-, and 6-fold drop in potency, respectively, if compared with their relatives 24, 28, and 35 that were not substituted at C(6).

Acidic compounds tend to bind to basic serum albumin. Therefore, not surprisingly the compounds discussed herein displayed high plasma protein binding in an in vitro plasma protein binding assay (PPB > 97%, data not shown). Since targeted *h*CRTh2 is located on circulating cells, the impact of plasma protein binding on the potency of the *h*CRTh2 antagonists was assessed by adding 0.5% human serum albumin (HSA) to the binding assay buffer. Generally, a less than 10-fold HSA shift factor *f*_{HSA}, defined as the ratio IC₅₀(HSA)/IC₅₀(buffer), was noticed. With the exceptions of 30 and 31, a substantially higher albumin shift up to a factor *f*_{HSA} of 57 was observed in the cases where R was a naphthyl or a naphthylmethyl moiety. No obvious correlation between *f*_{HSA} and physicochemical parameters of the antagonists (Table 3) could be established. However, a comparable shift effect was observed for the inhibition of the PGD₂ induced morphological shape change of human eosinophils measured in the presence of human plasma.

Since agonistic activity on the CRTh2 receptor was reported for structurally related indolylacetic acid 2,¹⁸ 2-(3,4-dihydro-1*H*-pyrido[4,3-*b*]indol-5(2*H*)-yl)acetic acid derivatives 5 and 11–36 were consequently tested for their agonistic potential. It could be demonstrated that all compounds were solely antagonists on *h*CRTh2, fully antagonizing the PGD₂ induced

effects with the IC₅₀ values given in Table 2 for both cell based functional assays, the Ca²⁺ flux and the cAMP assay. Moreover, species selectivity was addressed in a concomitant study by testing the compounds in a FLIPR assay against mouse, rat, guinea pig, and dog CRTh2 using cells expressing the respective recombinant species CRTh2. Antagonistic effects with comparable potencies were found as for *h*CRTh2 except for 24, 26, and 28. Unexpectedly, these three examples were identified as partial agonists on the mouse and the guinea pig receptor (data not shown), limiting the choice of potential in vivo animal models for efficacy studies.

In addition, all antagonists inhibited the PGD₂ induced shape change of human eosinophils in the *h*ESC assay. Compounds 22–24 and 33 were discovered to antagonize *h*ESC most effectively with IC₅₀ < 100 nM. In fact, these antagonists belong to the group that exhibited only a minor serum albumin shift *f*_{HSA} in the binding assay.

Selectivity against other prostanoid receptors was considered important in order to avoid unwanted adverse effects from off-target effects. All compounds were tested against the human PGD₂ receptor *h*DP₁, the human PGE₂ receptors *h*EP₁, *h*EP₂, *h*EP₃, and *h*EP₄, and the human TXA₂ receptor *h*TP₂. Many of the antagonists were highly selective with a selectivity factor *f*_{sel} > 1000 in favor of *h*CRTh2 (Table 2). However, a few antagonists were identified that manifested considerable affinities in the low micromolar to submicromolar range for the *h*DP₁ receptor. Those compounds could be classified mainly into two groups. For example, molecules where R¹ is representing a chlorine atom connected to C(6), as exemplified with 25, 31, and 36, could be assigned to one group. In these cases, a selectivity factor *f*_{sel} in the range between 4 and 20 was obtained. This narrow selectivity window originates from an up to 20-fold loss in potency for *h*CRTh2 on one hand and from a considerable gain in affinity for the *h*DP₁ receptor on the other. The second group contained molecules with R representing the large lipophilic naphthyl, as illustrated with 26–30, or biphenyl, exemplified by 35. These compounds were identified as being highly potent on *h*CRTh2 but were also found to inhibit the *h*DP₁ receptor in the low micromolar to submicromolar range, resulting in a selectivity factor in the range 80 < *f*_{sel} < 1000. A selectivity factor of *f*_{sel} > 200 in favor of *h*CRTh2 was applied as a selection criterion in order to further profile a compound. Some minor cross-selectivity was observed in the single digit micromolar range with PGE₂ receptor *h*EP₂ measured in the β-arrestin assay (IC₅₀ > 10 μM in the binding assay); however, the selectivity factors *f*_{sel} were all >400 in favor of the CRTh2 antagonists (Table 2). The compounds were found to be highly selective against the other EP receptors (*h*EP₁, IC₅₀ > 25 μM

(Ca²⁺); hEP₃, IC₅₀ > 25 μM (Ca²⁺); hEP₄, IC₅₀ > 10 μM (β-arrestin and binding). In contrast to structurally related **3**, no inhibition of hTP₂ receptor was observed for this compound series (IC₅₀ > 25 μM (Ca²⁺)).

The inhibitory potential of 2-(3,4-dihydro-1H-pyrido[4,3-b]indol-5(2H)-yl)acetic acid analogues **5** and **11–36** for enzymes that are involved in the prostaglandin synthesis, for example, the COX enzymes, was addressed because of the structural similarity with NSAID **2**, a nonselective COX inhibitor.¹⁷ All hCRTh2 antagonists reported herein reduced COX-1 enzyme activity by less than 30% at 10 μM compound concentration (no detailed data shown); hence, all IC₅₀ values were determined well above 10 μM.

Physicochemical and in Vitro ADME Properties.

Physicochemical properties of the antagonists selected for further profiling are given in Table 3. The molecular weights were all below 450 Da, in an optimal range between 358 and 438 Da as targeted for small druglike molecules. Furthermore, the attractive ligand efficiencies (LE) with values between 0.35 and 0.46 placed the compounds in the envisaged range of that for oral drug candidates.²⁹ The cLogP values were calculated between 2.0 and 4.4 as a measure of molecular hydrophobicity, and these values were well below 5, in accordance with Lipinski's rule of five.³⁰ Generally, the low to medium molecular weights (MWs) ranging from 358 to 416 Da, cLogP values between 2.0 and 3.3, and log *D*_{7.4} values ranging from -0.3 to +0.2 provided compounds that were highly soluble in buffered aqueous solution at pH 7 with solubility values between 560 and 1000 μg/mL. Still an acceptable solubility was obtained in buffer at pH 4 (21–180 μg/mL) or even in pure water (25–335 μg/mL). Unsurprisingly, the most hydrophobic compound **35** listed in Table 3 displayed the highest cLogP value of 4.4 and the highest log *D*_{7.4} value of 1.8 in this series and consequently was found to be insoluble in buffer at pH 4 and water (1 and 2 μg/mL, respectively). Only poor solubility was measured in buffer at pH 7 (30 μg/mL).

The drug–drug interaction potential for the selected antagonists in Table 4 was assessed in vitro by measuring the inhibition of the cytochrome P450 isoforms 2C9, 2D6, and 3A4. Since all IC₅₀ values were well above 10 μM, a low drug–drug interaction potential was considered for those compounds.

Chemical stability in various media was evaluated by incubating the compounds in rat and human plasma for up to 4 h, in simulated gastric fluid (SGF) for 1 h, and in simulated

Table 4. In Vitro ADME Properties of Selected Potent Antagonists in Comparison with Lead Compound **5**

compd	CYP2C9 ^a IC ₅₀ (μM)	Cl _{int} ^{int} (μL min ⁻¹ (mg protein) ⁻¹)		Cl _{int} (μL min ⁻¹ (10 ⁶ cells) ⁻¹), RHepa
		HLM	RLM	
5	15	5	<4	0.9
22	43	<4	8	2.1
23	>50	5	24	1.4
24	>50	<4	<4	1.9
26	40	<4	36	1.5
28	>50	5	5	3.1
32	16	6	63	nd
33	>50	<4	23	nd
35	14	85	31	5.3

^aCYP inhibition: IC₅₀(2D6,3A4) > 50 μM.

intestinal fluid (SIF) for 4 h.³¹ Recovery of unchanged parent compound was determined by LC–MS. The compounds were stable under the described conditions. The elimination half-life (*T*_{1/2}) was found to be >4 h after exposure in rat as well as in human plasma, and *T*_{1/2} > 1 h in SGF, and *T*_{1/2} > 4 h in SIF (see Supporting Information).

Metabolic stability was assessed by incubating the compounds with human and rat liver microsomes as well as with plated rat hepatocytes (Table 4). With the exception of **35** all compounds displayed a very low intrinsic clearance (Cl_{int}) with values below 10 μL min⁻¹ (mg protein)⁻¹ after incubation with human liver microsomes. An increased clearance (Cl_{int} = 85 μL min⁻¹ (mg protein)⁻¹) was observed for **35**. Only **22**, **24**, and **28** provided similarly low Cl_{int} values in rat liver microsomes, whereas **23**, **26**, **32**, **33**, and **35** were found to be more prone to oxidative metabolism, providing Cl_{int} values in the range between 23 and 63 μL min⁻¹ (mg protein)⁻¹. A low clearance was observed in rat hepatocytes with all Cl_{int} values not exceeding 5.3 μL min⁻¹ (10⁶ cells)⁻¹.

In Vivo Pharmacokinetic Studies. Pharmacokinetic studies with a representative set of potent and selective CRTh2 antagonists (Table 5) were carried out in the Wistar rat

Table 5. Pharmacokinetic Profile of Selected Potent Antagonists, Determined in Male Wistar Rats (Three Animals for Each Experiment) after Intravenous (iv) and Oral (po) Administrations as Solutions^a

compd	AUC _{0–last} (ng h ⁻¹ mL ⁻¹)	CL (mL min ⁻¹ kg ⁻¹)	<i>T</i> _{1/2} (h)	<i>F</i> (%)
5	6300	4.6	2.3	14
22	244	36	0.6	5
24	6450	5.9	2.3	23
26	57300	1.1	5.8	36
28	58500	1.3	6	44
33	62	11	1.2	2
35	171	35	0.5	4

^a*V*_{ss} = 0.4–0.8 L/kg for all compounds tested. iv: 2 mg/kg (**28**, **35**), 1 mg/kg (**5**, **22**, **24**, **26**), 0.2 mg/kg (**33**). po: 10 mg/kg (**5**, **22**, **24**, **26**, **28**, **35**), 2 mg/kg (**33**).

at intravenous doses of 0.2, 1, and 2 mg/kg and at oral doses of 2 and 10 mg/kg. Among the six antagonists presented, **28** and its des-fluoro analogue **26** displayed the most favorable pharmacokinetic properties with an excellent exposure (AUC_{0–last}) of 58 500 and 57 300 ng h⁻¹ mL⁻¹, low plasmatic clearance of 1.3 and 1.1 mL min⁻¹ kg⁻¹, and an oral bioavailability of 44% and 36%, respectively. In comparison, a 5-fold higher plasma clearance was observed for **24**. Indeed, despite low plasmatic clearance of 5.9 mL min⁻¹ kg⁻¹, only a moderate exposure of 6450 ng h⁻¹ mL⁻¹ was determined, leading to an oral bioavailability of 23%. With **33**, the exposure dropped to 62 ng h⁻¹ mL⁻¹, giving rise to a bioavailability of only 2%. The moderate plasmatic clearance of 11 mL min⁻¹ kg⁻¹ was not considered the only parameter attributed to the low bioavailability of **33**. Other additional effects like incomplete absorption or active secretion into the gut lumen could also be reasons for the low bioavailability. Compounds **22** and **35** displayed the highest clearance within this series, with values of 35 and 36 mL min⁻¹ kg⁻¹. Consequently, their exposures were well below 500 ng h⁻¹ mL⁻¹ and their respective oral bioavailability did not exceed the 5% threshold. For all the antagonists tested, a low volume of distribution *V*_{ss}

typical for acidic drugs (e.g., warfarin, aspirin) was found within a range of 0.4–0.8 L/kg.

Pharmacokinetic studies with **24** and **28** were performed in male Beagle dogs. Both compounds were administered orally at a dose of 10 mg/kg and intravenously at a dose of 1 mg/kg as solutions containing 10% propylene glycol (PG). The acquired data are presented in Table 6. The exposure after oral

Table 6. Pharmacokinetic Profile of **24 and **28** Determined in Male Beagle Dogs (Three Animals for Each Experiment) after Intravenous and Oral Administrations at a Dose of 1 and 10 mg/kg, Respectively**

compd	AUC _{0–last} (ng h ⁻¹ mL ⁻¹)	CL _{iv} (mL min ⁻¹ kg ⁻¹)	F (%)
24	9620	11	64
28	91100	1.3	55

administration of **24** and **28** was higher than in the rat with values of 9620 and 91 100 ng h⁻¹ mL⁻¹, respectively. Both compounds showed a similar bioavailability with 55% for **28** and 64% for **24** despite a 10-fold difference in plasmatic clearance after intravenous administration. Indeed, while **28** was found to be a low clearance compound with a value of 1.3 mL min⁻¹ kg⁻¹, the clearance for **24** was elevated to 11 mL min⁻¹ kg⁻¹.

Discussion. The optimization program of the 2-(3,4-dihydro-1*H*-pyrido[4,3-*b*]indol-5(2*H*)-yl)acetic acid lead series with the main focus on the improvement in potency and oral bioavailability offered numerous *h*CRTh2 antagonists with interesting characteristics. A visualization device was considered useful in order to simplify a data-driven analysis of the collected data and to evaluate and prioritize candidates showing a balanced profile with a great promise for further development. Therefore, a traffic light (TL) selection tool,³² basically a conditional formatting with the color coding red, yellow, and green, was applied (Table 7). Threshold ranges were defined

Table 7. Applying Traffic Lights (TL) as a Tool for the Data-Driven Selection of the Clinical Candidate^a

	TL CRTh2 Bdg IC ₅₀	TL albumin shift <i>f</i> _{HSA}	TL FLIPR IC ₅₀	TL cAMP IC ₅₀	TL <i>h</i> ESC IC ₅₀	TL Selectivity <i>f</i> _{sel}	TL Exposure ng h ⁻¹ ml ⁻¹	TL T _{1/2} [h]
5	15	1	170	190	110	>700	6300	2.3
24	7	10	23	95	57	>1100	6450	2.3
26	9	60	30	140	1120	87	57300	5.8
28	6	57	28	80	235	215	58500	6
Threshold range	<10	<10	<100	<100	<100	>500	>10000	>5
	>20	>100	>250	>250	>250	<100	<1000	<1

^aColor coded thresholds (green, go; yellow, alert; red, no go) are given for selected properties of antagonist **24**, **26**, and **28** in comparison with lead compound **5**.

and applied for the more than 30 parameters that were presented throughout Tables 2–6 and discussed in the corresponding paragraphs. A red TL was used to visualize values in a less favored range as a “no go”. A yellow TL was set as an alert for moderate data, whereas a green TL was employed to highlight a “go” for excellent parameter data. The threshold ranges were applied on the full data set of eligible antagonists. However, only the eight parameters that differed most for **5**, **24**, **26**, and **28** were listed in Table 7 as TLs,

including their respective threshold ranges; the TLs of the remaining parameters were not registered in Table 7 because they all appeared in the green range for the best candidates. This assessment revealed that lead structure **5** already displayed a favorable and overall druglike profile. No red flags appeared, and only 6 out of the 33 parameters really offered potential room for improvement (Table 7). Applying the threshold ranges with the respective color coding uncovered not more than three close analogues (**24**, **26**, and **28**) with more green TLs than **5**. Ultimately, the envisaged optimization effort concluded with the three potential candidates **24**, **26**, and **28**. For example, four parameters of **26** were clearly improved, as shown with four yellow TL changing to green. However, at the same time three other parameters changed for the worse; for example, the TL for *f*_{HSA} changed from green to yellow, the TL *f*_{sel} from green to red, and TL *h*ESC from yellow to red. More importance was attached to the worsening of the last two parameters, especially the shift toward much lower potency with IC₅₀ > 1 μM in the relevant functional *h*ESC assay, than to the positive almost 10-fold improved exposure, and thus, **26** was not considered a probable candidate. Actually, antagonist **24** was identified as the most balanced candidate with the most green, the least yellow, and with no red TLs. Example **28** scored second with one yellow TL more for the serum albumin shift factor *f*_{HSA}. A closer look at the TL alert for *h*ESC of **28** revealed a 4-fold drop in potency if compared with **24**. However, by comparison of the plasma exposure of **28** (green TL) with **24** (yellow TL), it became obvious that **28** outperformed **24** by a factor of 10 in this respect, thus compensating the aforementioned 4-fold potency drop by more than a factor of 2. Well knowing that the shift to lower potency in plasma and consequently in whole blood could compromise in vivo efficacy, **28** was nevertheless selected for further development mainly because of its excellent oral uptake and the high exposure that could be reached. It was believed that therapeutically relevant drug levels still could be obtained, especially at higher dosage. The full pharmacokinetic and pharmacodynamic profile of **28** will be presented in a forthcoming publication.

CONCLUSIONS

In summary, an optimization process with the main focus to improve potency and oral bioavailability of a novel *h*CRTh2 antagonist series was presented starting with the recently disclosed 2-(2-(1-naphthoyl)-8-fluoro-3,4-dihydro-1*H*-pyrido[4,3-*b*]indol-5(2*H*)-yl)acetic acid **5** as lead compound. Data were collected on more than 30 parameters for a set of about 200 newly synthesized analogues. A traffic light analysis was conducted to visualize and to compare the data and to evaluate and prioritize candidates displaying a balanced profile. This data-driven process and the excellent results of the PK study in the rat (*F* = 44%) and the dog (*F* = 55%) facilitated the identification of 2-(2-(1-naphthoyl)-8-fluoro-3,4-dihydro-1*H*-pyrido[4,3-*b*]indol-5(2*H*)-yl)acetic acid **28** (setipiprant/ACT-129968) as a potent, selective, and orally available *h*CRTh2 antagonist. Unfortunately, it was not feasible to rely on the efficacy in animal asthma models as a selection criterion for the development candidate because the most balanced *h*CRTh2 antagonists **24**, **26**, and **28** turned out to act as partial agonists on the mouse or guinea pig receptor. This fact limited the choice of animal asthma models. For that reason and because of the complex challenges concerning the in vivo pharmacological profiling of **28** in animal models as well as the cell based in vitro

studies with cells originating from various species, no further particulars on pharmacological data were discussed herein. These data will be presented and discussed in a dedicated publication (paper in preparation). Since the treatment of patients has been the ultimate goal, selection priority was based on the activity of the antagonists on relevant CRTh2 expressing human cells and oral bioavailability. Ultimately, **28** was selected for further studies and proposed as a clinical development candidate for the treatment of asthma and seasonal allergic rhinitis. At the time of selection, **28** was among the first *h*CRTh2 antagonists available, and therefore, we decided to commence clinical profiling in order to obtain proof of concept for CRTh2 inhibition in humans, to evaluate safety aspects, and to gain further experience with such a novel treatment modality, however, being well aware of the fact that the observed blood plasma shift to lower potency, especially in the more important cellular test systems, could compromise the outcome of clinical efficacy. Therapeutically relevant drug levels were expected to be reached, especially at higher dosage, because of the excellent oral uptake of **28** and hence its high systemic exposure. Moreover, in the course of our subsequent discovery and development efforts more emphasis was put on the plasma protein effect in order to identify antagonists with highly potent inhibitory activity on CRTh2 expressing human cells and exhibiting no or only a minor shift to lower potency in the presence of human blood plasma and human whole blood. The clinical program and the generated novel understanding concerning CRTh2 antagonism in human volunteers and patients will be discussed in future reports.

EXPERIMENTAL SECTION

Reagents and solvents were used as purchased without any further purification. Reactions were performed under inert Ar or N₂ atmosphere unless stated otherwise. NMR data were recorded at room temperature on a Bruker Avance II 400 MHz spectrometer equipped with a BBO 5 mm probe head unless stated otherwise. Chemical shifts (δ) are reported in parts per million (ppm) relative to proton resonances resulting from incomplete deuteration of the NMR solvent, e.g., for dimethylsulfoxide δ (H) 2.49 ppm, for chloroform δ (H) 7.24 ppm. The abbreviations s, d, t, q, m, and b refer to singlet, doublet, triplet, quartet, multiplet, and broad, respectively.

The following instruments and conditions were used. For analytical LC(1)/ESI-MS: Dionex HPG-3200RS pump system; MS, Thermo MSQ Plus MS detector; (DAD)/ (ELSD), DAD-3000RS detector equipped with Sedere Sedex 85 ELS detector; column, Zorbax SB-Aq, 3.5 μ m, 4.6 mm \times 50 mm, 40 $^{\circ}$ C; eluent A, water containing 0.04% TFA; eluent B, acetonitrile; gradient, 5–95% B over 1 min; flow rate, 4.5 mL/min. For analytical LC(2)/ESI-MS: Dionex HPG-3200RS pump system; MS, Thermo MSQ Plus MS detector; DAD/ELSD, DAD-3000RS detector equipped with Sedere Sedex 85 ELS detector; column, Atlantis T3, 5 μ m, 4.6 mm \times 30 mm, 40 $^{\circ}$ C; eluent A, water containing 0.04% TFA; eluent B, acetonitrile; gradient, 5–95% B over 1 min; flow rate, 4.5 mL/min. For analytical LC(3)/ESI-MS: Waters Acquity binary pump system; MS, Waters Aquity SQD; DAD/ELSD, Waters Acquity PDA and ELS detector; column, UPLC BEH C18 1.7 μ m, 2.1 mm \times 50 mm; eluent A, water containing 0.05% formic acid; eluent B, acetonitrile containing 0.05% formic acid; gradient, 2–95% B over 1.4 min and then 95–98% B over 0.4 min; flow rate, 1.2 mL/min. For preparative HPLC: Gilson 333/334 binary high pressure gradient pump system equipped with Sedere Sedex V.F.S variable flow splitter, Dionex P680 isocratic make-up pump; DAD, Dionex UVD340U DAD detector; MS, Finnigan AQA MS detector; fraction collection, Gilson 215 autosampler and fraction collector; column, Atlantis Prep C18 (30 mm \times 75 mm OBD); eluent A, water containing 0.05% formic acid; eluent B, acetonitrile; flow rate, 75 mL/min. For HR-LC-MS: Waters Acquity binary pump system, solvent manager; MS, SYNAPT G2MS;

source temperature, 150 $^{\circ}$ C; desolvation temperature, 400 $^{\circ}$ C; desolvation gas flow, 400 L/h; cone gas flow, 10 L/h; extraction cone, 4 RF; lens, 0.1 V; sampling cone, 30; capillary, 1.5 kV; high resolution mode; gain, 1.0; MS function, 0.2 s per scan; 120–1000 amu in full scan, centroid mode; lock spray, leucine enkephalin 2 ng/mL (556.2771 Da); scan time, 0.2 s with interval of 10 s and average of 5 scans; DAD, Acquity UPLC PDA detector; column, Waters Acquity UPLC BEH C18, 1.7 μ m, 2.1 mm \times 50 mm, thermostated in the Acquity UPLC column manager at 60 $^{\circ}$ C; eluent A, water containing 0.05% formic acid; eluent B, acetonitrile containing 0.05% formic acid; gradient, 2–98% B over 3.0 min; flow rate, 0.6 mL/min; detection, UV 214 nm and MS. Melting points were measured on a Sanyo Gallenkamp digital apparatus and are uncorrected.

All compounds tested for biological activity are reported as having at least 95% purity as judged by HPLC method LC(1).

General Procedure for the Synthesis of 7a–I (Scheme 1, Stage a). To suspensions of the respective 2,3,4,5-tetrahydro-1*H*-pyrido[4,3-*b*]indole hydrochloride salts **6a–I** (18.4 mmol) in DCM (100 mL) were added DIPEA (22.1 mmol, 2.85 g, 3.78 mL) and di-*tert*-butyl dicarbonate (19.3 mmol, 4.22 g). The resulting white solutions were allowed to stir at ambient temperature for 1 h. Saturated aqueous NH₄Cl solution was added, and the resulting aqueous phases were extracted twice with DCM. The combined organic phases were washed with water and brine and then dried over MgSO₄. The solvent was evaporated in vacuo, and the resulting solids were dried under high vacuum and used as such in the next step.

tert-Butyl 3,4-Dihydro-1*H*-pyrido[4,3-*b*]indole-2(5*H*)-carboxylate (7a, R¹ = H).³³ Boc protection of **6a** provided **7a** as a white solid in 83% yield. LC(1)/ESI-MS t_R = 1.00 min; m/z [M + H⁺] = 273.07. ¹H NMR (CDCl₃) δ : 7.83 (s), 7.45 (d, J = 7.3 Hz, 1 H), 7.31 (m, 1 H), 7.13 (m, 2 H), 4.64 (s, 2 H), 3.82 (bs, 2 H), 2.83 (bs, 2 H), 1.50 (s, 9 H). HRMS (ESI): m/z calcd for C₁₆H₂₁N₂O₂ [M + H⁺] 273.1603, found 273.1598.

tert-Butyl 8-Fluoro-3,4-dihydro-1*H*-pyrido[4,3-*b*]indole-2(5*H*)-carboxylate (7b, R¹ = 8-F).^{34,35} Boc protection of **6b** provided **7b** as a brown solid in 96% yield. LC(1)/ESI-MS t_R = 0.91 min; m/z [M + H⁺] = 291.20. ¹H NMR (DMSO-*d*₆) δ : 10.99 (s, 1 H), 7.28 (dd, J_1 = 8.8 Hz, J_{H-F} = 4.5 Hz, 1 H), 7.18 (dd, J_{H-F} = 9.9 Hz, J_2 = 2.4 Hz, 1 H), 6.86 (ddd, J_{H-F} = 9.9 Hz, J_1 = 8.8 Hz, J_2 = 2.4 Hz, 1 H), 4.50 (s, 2 H), 3.70 (t, J = 5.7 Hz, 2 H), 2.78 (t, J = 5.7 Hz, 2 H), 1.45 (s, 9 H). HRMS (ESI): m/z calcd for C₁₆H₂₀N₂O₂F [M + H⁺] 291.1509, found 291.1515.

General Procedure for the Synthesis of 8a–I (Scheme 1, Stage b). To solutions of the respective *tert*-butyl 3,4-dihydro-1*H*-pyrido[4,3-*b*]indole-2(5*H*)-carboxylate derivatives **7a–I** (1.17 mmol) and ethyl bromoacetate (1.4 mmol, 239 mg, 0.159 mL) in DMF (3 mL) was added Cs₂CO₃ (2.34 mmol, 761 mg). The resulting reaction mixtures were allowed to stir at 80 $^{\circ}$ C for 1 h. After the mixtures were cooled, 10 mL of water and 10 mL of brine were added and the resulting aqueous phases were extracted three times with DCM. The combined organic phases were washed with water and brine and dried over MgSO₄. Evaporation of the solvent in vacuo yielded brown pastes from which the pure products **8a–I** were isolated by flash chromatography on silica gel using EtOAc/*n*-heptane as eluent or by precipitation from cyclohexane.

For the preparation of **8b**, **8d**, and **8i**, acetone was used as solvent instead of DMF and the reaction was performed at room temperature.

tert-Butyl 5-(2-Ethoxy-2-oxoethyl)-3,4-dihydro-1*H*-pyrido[4,3-*b*]indole-2(5*H*)-carboxylate (8a, R¹ = H).³⁶ Alkylation of **7a** provided **8a** as a yellow oil in 58% yield. LC(1)/ESI-MS t_R = 0.97 min; m/z [M + H⁺] = 359.29. ¹H NMR (CD₃OD) δ : 7.42 (d, J = 7.7 Hz, 1 H), 7.26 (m, 1 H), 7.15 (m, 1 H), 7.07 (m, 1 H), 4.89 (s, 2 H), 4.62 (s, 2 H), 4.19 (q, J = 7.3 Hz), 3.83 (t, J = 5.6 Hz, 2 H), 2.76 (t, J = 5.6 Hz, 2 H), 1.52 (m, 9 H), 1.26 (t, J = 7.1 Hz, 3 H). ¹³C NMR (CD₃OD) δ : 169.4, 155.6 (bs), 137.1, 133.6 (bs), 125.5, 121.1, 119.2, 117.0, 108.5, 106.9 (bs), 80.1, 61.2, 43.8, 41.6–40.5 (m), 27.4, 21.7 (bs), 13.1. HRMS (ESI): m/z calcd for C₂₀H₂₇N₂O₄ [M + H⁺] 359.1971, found 359.1977.

tert-Butyl 5-(2-Ethoxy-2-oxoethyl)-8-fluoro-3,4-dihydro-1*H*-pyrido[4,3-*b*]indole-2(5*H*)-carboxylate (8b, R¹ = 8-F).³⁷ Alkyl-

tion of **7b** provided **8b** after precipitation from cyclohexane as a white solid in 70% yield. LC(1)/ESI-MS $t_R = 0.97$ min; m/z $[M + H^+] = 377.20$. 1H NMR ($CDCl_3$) δ : 7.13 (m, 2 H), 6.94 (td, $J_{H-F} = 9.1$ Hz, $J_1 = 9.1$ Hz, $J_2 = 2.3$ Hz, 1 H), 4.73 (s, 2 H), 4.62 (bs, 2 H), 4.23 (q, $J = 7.1$ Hz, 2 H), 3.87 (bs, 2 H), 2.77 (bs, 2 H), 1.53 (s, 9 H), 1.29 (t, $J = 7.1$ Hz, 3 H). ^{13}C NMR ($CDCl_3$): δ 168.4, 158.0 (d, $J_{C-F} = 235$ Hz), 155.1 (bs), 135.5 (m), 133.4, 125.9 (m), 109.5 (d, $J_{C-F} = 26$ Hz), 109.2 (d, $J_{C-F} = 10$ Hz), 108.1 (m), 103.3 (d, $J_{C-F} = 24$ Hz), 80.0, 61.8, 44.8, 41.1–40.4 (m), 28.5, 22.5 (bs), 14.2. HRMS (ESI): m/z calcd for $C_{20}H_{26}N_2O_4F$ $[M + H^+] 377.1876$, found 377.1871.

General Procedure for the Synthesis of 9a–I (Scheme 1, Stage c). To solutions of the respective *tert*-butyl 5-(2-ethoxy-2-oxoethyl)-3,4-dihydro-1H-pyrido[4,3-*b*]indole-2(*SH*)-carboxylate derivatives **8a–I** (2 mmol) in DCM (5 mL) were added dropwise a solution of 4 N HCl in 1,4-dioxane (5 mL) at ambient temperature. The resulting mixtures were allowed to stir at ambient temperature for 3 h. Then the solvents were removed under reduced pressure and the crude solids were dried under high vacuum and used without further purification in the next step.

Ethyl 2-(3,4-Dihydro-1H-pyrido[4,3-*b*]indol-5(2H)-yl)acetate Hydrochloride (9a). Deprotection of **8a** provided **9a** as a white solid in 88% yield. LC(1)/ESI-MS $t_R = 0.59$ min; m/z $[M + H^+] = 259.28$. 1H NMR (CD_3OD) δ : 7.50 (d, $J = 7.8$ Hz, 1 H), 7.36 (m, 1 H), 7.23 (t, $J = 7.7$ Hz, 1 H), 7.14 (t, $J = 7.6$ Hz, 1 H), 5.01 (s, 2 H), 4.47 (s, 2 H), 4.23 (q, $J = 7.1$ Hz, 2 H), 3.66 (m, 2 H), 3.13 (t, $J = 6.1$ Hz, 2 H), 1.29 (t, $J = 7.1$ Hz, 4 H).

Ethyl 2-(8-Fluoro-3,4-dihydro-1H-pyrido[4,3-*b*]indol-5(2H)-yl)acetate Hydrochloride (9b). Deprotection of **8b** provided **9b** as a white solid in 96% yield. LC(1)/ESI-MS $t_R = 0.63$ min; m/z $[M + H^+] = 277.22$. 1H NMR ($DMSO-d_6$) δ : 9.52 (m, 2 H), 7.46 (dd, $J_1 = 9.2$ Hz, $J_{H-F} = 4.4$ Hz, 1 H), 7.34 (dd, $J_{H-F} = 9.7$ Hz, $J_1 = 2.5$ Hz, 1 H), 7.00 (td, $J_{H-F} = 9.3$ Hz, $J_1 = 9.2$ Hz, $J_2 = 2.6$ Hz, 1 H), 5.12 (s, 2 H), 4.30 (bs, 2 H), 4.16 (q, $J = 7.1$ Hz, 2 H), 3.48 (s, 2 H), 2.99 (t, $J = 5.9$ Hz, 2 H), 1.23 (t, $J = 7.1$ Hz, 3 H).

General Procedure for the Synthesis of 10a₁ to 10_l (Scheme 1, Stage d). To cooled suspensions of the respective ethyl 2-(3,4-dihydro-1H-pyrido[4,3-*b*]indol-5(2H)-yl)acetate hydrochloride salts **9a–I** (7 mmol) in DCM (20 mL) was added DIPEA at 0 °C (21 mmol), followed by the corresponding acyl chlorides (7.7 mmol). The resulting brown suspensions were allowed to stir at room temperature for 1 h. DCM was added, and the resulting organic phases were first washed with saturated aqueous $NaHCO_3$ solution, then with water and brine. The combined organic phases were dried over $MgSO_4$ and yielded brown solids after evaporation of the solvent in vacuo. The crude products were purified by flash chromatography on silica gel, using $EtOAc/n$ -heptane as eluent. The various purification methods are mentioned within the corresponding sections.

Ethyl 2-(2-Benzoyl-3,4-dihydro-1H-pyrido[4,3-*b*]indol-5(2H)-yl)acetate (10a₁). Acylation of **9a** with benzoyl chloride provided **10a₁** after preparative HPLC purification as a beige solid in 70% yield. LC(1)/ESI-MS $t_R = 0.89$ min; m/z $[M + H^+] = 363.11$. 1H NMR ($CDCl_3$) δ : 7.40–7.61 (m, 5 H), 7.02–7.32 (m, 3 H), 5.01 (bs, 1 H), 4.78 (s, 2 H), 4.70 (bs, 1 H), 4.24 (q, $J = 7.1$ Hz, 3 H), 4.22 (bs, 1H), 3.81 (bs, 1 H), 2.79–3.00 (m, 2 H), 1.30 (t, $J = 7.1$ Hz, 3 H).

Ethyl 2-(2-(1-Naphthoyl)-3,4-dihydro-1H-pyrido[4,3-*b*]indol-5(2H)-yl)acetate (10a₃). Acylation of **9a** with 1-naphthoyl chloride provided crude **10a₃** as yellow solid in 97% yield. LC(1)/ESI-MS $t_R = 1.14$ min; m/z $[M + H^+] = 413.16$. 1H NMR ($DMSO-d_6$), 60:40 mixture of two rotamers, δ : 8.02 (m, 2 H), 7.76 (m, 1 H), 7.64–7.40 (m, 5.4 H), 7.37 (d, $J = 8.2$ Hz, 0.4 H), 7.16 (m, 0.6 H), 7.10 (m, 0.6 H), 7.03 (m, 0.6 H), 6.84 (t, $J = 7.4$ Hz, 0.4 H), 5.10 (s, 0.8 H), 4.99 (m, 2.2 H), 4.36 (m, 1 H), 4.19 (m, $J = 7.1$ Hz, 0.8 H), 4.14 (q, $J = 7.1$ Hz, 1.2 H), 4.08 (m, 0.8 H), 3.51 (t, $J = 5.6$ Hz, 1 H), 2.97 (m, 1 H), 2.68 (m, 1 H), 2.55 (m, 1 H), 1.25 (t, $J = 7.1$ Hz, 1.2 H), 1.19 (t, $J = 7.1$ Hz, 1.8 H). The compound was used without further purification in the next step.

Ethyl 2-(2-(4'-Ethyl-[1,1'-biphenyl]-4-carbonyl)-3,4-dihydro-1H-pyrido[4,3-*b*]indol-5(2H)-yl)acetate (10a₄). Acylation of **9a** with 4'-ethyl-[1,1'-biphenyl]-4-carbonyl chloride provided **10a₄** after column chromatography on silica gel, using $EtOAc/n$ -heptane as

eluent, as a white solid in 67% yield. LC(1)/ESI-MS $t_R = 1.04$ min; m/z $[M + H^+] = 467.29$. 1H NMR ($DMSO-d_6$), 50:50 mixture of two rotamers, δ : 7.64 (m, 2.5 H), 7.56 (m, 4 H), 7.30 (d, $J = 7.5$ Hz, 3 H), 7.00–7.25 (m, 2.5 H), 4.98 (bs, 1 H), 4.77 (m, 3 H), 4.22 (m, 3 H), 3.86 (m, 1 H), 2.89 (m, 2 H), 2.71 (q, $J = 7.4$ Hz, 2 H), 1.28 (m, 6 H).

Ethyl 2-(2-(1-Naphthoyl)-8-fluoro-3,4-dihydro-1H-pyrido[4,3-*b*]indol-5(2H)-yl)acetate (10b₁). Acylation of **9b** with 1-naphthoyl chloride provided **10b₁** after precipitation from *n*-heptane as a brown solid in 98% yield. LC(1)/ESI-MS $t_R = 0.95$ min; m/z $[M + H^+] = 431.18$. 1H NMR ($DMSO-d_6$), 55:45 mixture of two rotamers, δ : 7.88–7.98 (m, 2.55 H), 7.85 (d, $J = 8.3$ Hz, 0.45 H), 7.44–7.59 (m, 4 H), 7.25 (dd, $J_{H-F} = 9.3$ Hz, $J_1 = 2.4$ Hz, 0.55 H), 7.17 (dd, $J_1 = 8.9$ Hz, $J_{H-F} = 4.2$ Hz, 0.55 H), 7.12 (dd, $J_1 = 8.8$ Hz, $J_{H-F} = 4.1$ Hz, 0.45 H), 7.00 (ddd, $J_{H-F} = 9.1$ Hz, $J_1 = 8.9$ Hz, $J_2 = 2.4$ Hz, 0.55 H), 6.89 (ddd, $J_{H-F} = 9.0$ Hz, $J_1 = 8.8$ Hz, $J_2 = 2.5$ Hz, 0.45 H), 6.74 (dd, $J_{H-F} = 9.3$ Hz, $J_2 = 2.5$ Hz, 0.45 H), 5.14 (m, 1.1 H), 4.78 (s, 0.9 H), 4.70 (s, 1.1 H), 4.30–4.48 (m, 1.8 H), 4.26 (q, $J = 7.3$ Hz, 0.9 H), 4.21 (q, $J = 7.0$ Hz, 1.1 H), 3.64 (t, $J = 5.7$ Hz, 1.1 H), 3.01 (m, 0.9 H), 2.65 (m, 1.1 H), 1.32 (t, $J = 7.1$ Hz, 1.35 H), 1.27 (m, 1.65 H).

Ethyl 2-(8-Fluoro-2-(thiophene-2-carbonyl)-3,4-dihydro-1H-pyrido[4,3-*b*]indol-5(2H)-yl)acetate (10b₃). Acylation of **9b** with thiophene-2-carbonyl chloride provided **10b₃** after precipitation from acetonitrile/diethylether as a white solid in 69% yield. LC(1)/ESI-MS $t_R = 1.09$ min; m/z $[M + H^+] = 386.96$. 1H NMR ($DMSO-d_6$) δ : 7.81 (dd, $J_1 = 5.0$ Hz, $J_2 = 1.0$ Hz, 1 H), 7.56 (m, 1 H), 7.43 (dd, $J_1 = 8.9$ Hz, $J_2 = 4.4$ Hz, 1 H), 7.32 (m, 1 H), 7.19 (dd, $J_1 = 5.0$ Hz, $J_2 = 3.7$ Hz, 1 H), 6.95 (ddd, $J_1 = 9.3$ Hz, $J_2 = 9.3$ Hz, $J_3 = 2.5$ Hz, 1 H), 5.08 (s, 2 H), 4.85 (m, 2 H), 3.99 (t, $J = 5.7$ Hz, 2 H), 2.90 (m, 2 H), 1.22 (t, $J = 7.1$ Hz, 3 H).

Ethyl 2-(2-(3-Chlorobenzoyl)-8-fluoro-3,4-dihydro-1H-pyrido[4,3-*b*]indol-5(2H)-yl)acetate (10b₄). Acylation of **9b** with 3-chlorobenzoyl chloride provided **10b₄** after precipitation from acetonitrile/diisopropylether as a white solid in 70% yield. LC(1)/ESI-MS $t_R = 1.04$ min; m/z $[M + H^+] = 415.11$. 1H NMR ($DMSO-d_6$), 53:47 mixture of two rotamers, δ : 7.40–7.47 (m, 1 H), 7.28–7.40 (m, 3 H), 7.08–7.20 (m, 1.53 H), 6.86–6.99 (m, 1.47 H), 5.06 (m, 0.53 H), 4.92 (m, 0.53 H), 4.74 (s, 0.94 H), 4.69 (m, 1.06 H), 4.49 (m, 0.47 H), 4.32–4.46 (m, 1 H), 4.22 (m, 2 H), 4.03 (ddd, $J_1 = 12.7$ Hz, $J_2 = 7.0$ Hz, $J_3 = 5.4$ Hz, 0.47 H), 3.66 (m, 1 H), 2.76–2.99 (m, 1.47 H), 2.70 (m, 0.53 H), 1.28 (t, $J = 7.3$ Hz, 1.41 Hz), 1.25 (t, $J = 7.0$ Hz, 1.59 Hz).

Ethyl 2-(2-(2-(1H-Indol-3-yl)acetyl)-8-fluoro-3,4-dihydro-1H-pyrido[4,3-*b*]indol-5(2H)-yl)acetate (10b₆). Acylation of **9b** with 2-(1H-indol-3-yl)acetyl chloride provided, after column chromatography on silica gel using $EtOAc/n$ -heptane as eluent, **10b₆** as a colorless resin in 81% yield. LC(1)/ESI-MS $t_R = 0.90$ min; m/z $[M + H^+] = 434.03$. 1H NMR ($CDCl_3$), 55:45 mixture of two rotamers, δ : 8.33 (m, 0.45 H), 8.12 (m, 0.55 H), 7.68 (m, 1 H), 7.37 (d, $J = 7.9$ Hz, 0.55 H), 7.05–7.28 (m, 4.45 H), 6.87–7.04 (m, 2 H), 4.84 (s, 0.9 H), 4.71 (s, 1.1 H), 4.68 (s, 1.1 H), 4.63 (s, 0.9 H), 4.21 (m, 2 H), 4.07 (t, $J = 5.5$ Hz, 1.1 H), 3.98 (s, 2 H), 3.83 (t, $J = 5.3$ Hz, 0.9 H), 2.79 (m, 1.1 H), 2.52 (s, 0.9 H), 1.27 (m, 3 H).

General Procedure for the Synthesis of 5 and 11–36 (Scheme 1, Stage e). To solutions of the respective esters **10a–I** (11 mmol) in THF (100 mL) was added 0.2 M aqueous NaOH solution (58 mL, 11.7 mmol). The resulting mixtures were allowed to stir at ambient temperature for 30 min. The reaction mixtures were extracted twice with diethyl ether. The pH of the aqueous phase was set to pH 2 by slow addition of concentrated aqueous HCl solution. The resulting acidic aqueous phases were extracted three times with DCM. The DCM phases were combined and dried over Na_2SO_4 . The volatiles were removed under reduced pressure, and the obtained solids were recrystallized from acetonitrile or purified by preparative HPLC.

2-(2-Benzoyl-3,4-dihydro-1H-pyrido[4,3-*b*]indol-5(2H)-yl)-acetic Acid (5). Saponification of **10a₁** provided pure **5** after recrystallization from acetonitrile as an orange solid in 73% yield, mp 225.8–226.9 °C (dec). LC(1)/ESI-MS $t_R = 0.77$ min; m/z $[M + H^+] = 335.06$. 1H NMR ($DMSO-d_6$), 60:40 mixture of two rotamers, δ : 13.04 (bs, 1 H), 7.44–7.57 (m, 5.6 H), 7.40 (m, 1 H), 7.27 (m, 0.4 H),

7.00–7.18 (m, 1.6 H), 6.97 (bs, 0.4 H), 4.94 (s, 2 H), 4.82 (bs, 1.2 H), 4.61 (bs, 0.8 H), 4.03 (bs, 0.8 H), 3.64 (bs, 1.2 H), 2.81 (s, 2 H). ^{13}C NMR (DMSO- d_6) δ : 170.9, 170.3 (bs), 137.2 (bs), 136.8 (bs), 134.2 (s), 130.1 (bs), 129.0, 127.5 (bs), 127.1 (bs), 121.5, 119.6, 118.0 (bs), 109.9, 106.4, 45.3 (bs), 45.1 (bs), 44.5, 22.9 (bs), 22.0 (bs). HRMS (ESI): m/z calcd for $\text{C}_{20}\text{H}_{19}\text{N}_2\text{O}_3$ [$\text{M} + \text{H}^+$] 335.1395, found 335.1396.

2-(2-(8-Fluoro-2-(thiophene-2-carbonyl)-3,4-dihydro-1H-pyrido[4,3-b]indol-5(2H)-yl)acetic Acid (22). Saponification of **10b₃** provided pure **22** after recrystallization from acetonitrile as a white solid in 82% yield, mp 239.4–241.9 °C (dec). LC(1)/ESI-MS t_{R} = 0.78 min; m/z [$\text{M} + \text{H}^+$] = 358.94. ^1H NMR (DMSO- d_6) δ : 13.09 (m, 1 H), 7.81 (dd, $J_1 = 5.0$ Hz, $J_2 = 0.7$ Hz, 1 H), 7.57 (d, $J = 0.3$ Hz, 1 H), 7.43 (dd, $J_1 = 8.9$ Hz, $J_2 = 4.4$ Hz, 1 H), 7.31 (d, $J = 8.8$ Hz, 1 H), 7.19 (dd, $J_1 = 4.9$ Hz, $J_2 = 3.8$ Hz, 1 H), 6.95 (ddd, $J_1 = 9.3$ Hz, $J_2 = 9.3$ Hz, $J_3 = 2.4$ Hz, 1 H), 4.97 (s, 2 H), 4.85 (bs, 2 H), 4.00 (t, $J = 5.6$ Hz, 2 H), 2.87 (s, 2 H). ^{13}C NMR (DMSO- d_6) δ : 170.8, 163.5, 157.6 (d, $J_{\text{C-F}} = 232$ Hz), 138.0, 136.6, 133.9, 130.3 (bs), 129.6 (bs), 127.8, 125.4 (d, $J_{\text{C-F}} = 10$ Hz), 110.9 (d, $J_{\text{C-F}} = 10$ Hz), 109.2 (d, $J_{\text{C-F}} = 26$ Hz), 106.7 (d, $J_{\text{C-F}} = 4$ Hz), 103.2 (d, $J_{\text{C-F}} = 24$ Hz), 44.7, 22.7 (bs). HRMS (ESI): m/z calcd for $\text{C}_{18}\text{H}_{16}\text{N}_2\text{O}_3\text{FS}$ [$\text{M} + \text{H}^+$] 359.0865, found 359.0863.

2-(2-(3-Chlorobenzoyl)-8-fluoro-3,4-dihydro-1H-pyrido[4,3-b]indol-5(2H)-yl)acetic Acid (24). Saponification of **10b₄** provided pure **24** after recrystallization from acetonitrile as a white solid in 89% yield, mp 251.8–256.2 °C (dec). LC(1)/ESI-MS t_{R} = 0.83 min; m/z [$\text{M} + \text{H}^+$] = 386.87. ^1H NMR (DMSO- d_6), 60:40 mixture of two rotamers, δ : 7.57 (m, 1 H), 7.50 (m, 2 H), 7.41 (d, $J = 7.5$ Hz, 1 H), 7.25–7.38 (m, 1.6 H), 7.03–7.17 (m, 0.4 H), 6.79–6.95 (m, 1 H), 4.78 (s, 1.2 H), 4.63 (s, 2 H), 4.56 (s, 0.8 H), 3.99 (s, 0.8 H), 3.64 (s, 1.2 H), 2.81 (m, 2 H). ^{13}C NMR (DMSO- d_6) δ : 170.8, 168.7 (bs), 157.6 (d, $J_{\text{C-F}} = 232$ Hz), 138.9 (bs), 138.6 (m), 136.9 (bs), 136.3 (bs), 133.9, 133.8, 131.0, 130.3–129.9 (m), 127.3 (bs), 127.0 (bs), 126.1 (bs), 125.7–125.2 (m), 110.9 (d, $J_{\text{C-F}} = 10$ Hz), 109.2 (d, $J_{\text{C-F}} = 26$ Hz), 106.5 (bs), 103.2 (d, $J_{\text{C-F}} = 24$ Hz), 45.1 (bs), 44.9 (bs), 44.7, 23.0 (bs), 22.6 (bs). HRMS (ESI): m/z calcd for $\text{C}_{20}\text{H}_{17}\text{N}_2\text{O}_3\text{ClF}$ [$\text{M} + \text{H}^+$] 387.0911, found 387.0910.

2-(2-(1-Naphthoyl)-3,4-dihydro-1H-pyrido[4,3-b]indol-5(2H)-yl)acetic Acid (26). Saponification of **10a₃** provided pure **26** after recrystallization from acetonitrile as a light yellow solid in 73% yield, mp 218.4–219.4 °C (dec). LC(1)/ESI-MS t_{R} = 0.82 min; m/z [$\text{M} + \text{H}^+$] = 385.03. ^1H NMR (DMSO- d_6), 65:35 mixture of two rotamers, δ : 13.03 (m, 1 H), 8.02 (m, 2 H), 7.75 (m, 1 H), 7.39–7.63 (m, 5.35 H), 7.36 (d, $J = 8.4$ Hz, 0.35 H), 7.15 (t, $J = 7.2$ Hz, 0.65 H), 7.09 (m, 0.65 H), 7.03 (m, 0.65 H), 6.83 (t, $J = 7.5$ Hz, 0.35 H), 5.06 (d, $J = 15.5$ Hz, 0.65 H), 4.99 (m, 1.35 H), 4.90 (m, 1.35 H), 4.42 (m, 0.35 H), 4.31 (m, 0.65 H), 4.08 (m, 0.35 H), 3.51 (t, $J = 5.4$ Hz, 1.35 H), 2.96 (m, 0.70 H), 2.68 (m, 0.65 H), 2.56 (m, 0.65 H). ^{13}C NMR (DMSO- d_6) δ : 170.9, 169.2, 137.3, 137.1, 135.2, 135.0, 134.1, 133.5, 133.5, 129.6, 129.5, 129.4, 129.3, 128.9, 128.9, 127.5, 127.0, 126.9, 126.0, 125.9, 125.5, 125.1, 125.0, 124.9, 124.1, 123.9, 121.6, 121.4, 119.7, 119.5, 118.0, 117.6, 109.9, 109.8, 106.5, 106.4, 44.6 (bs), 44.5, 39.3, 23.0, 22.2. HRMS (ESI): m/z calcd for $\text{C}_{24}\text{H}_{21}\text{N}_2\text{O}_3$ [$\text{M} + \text{H}^+$] 385.1552, found 385.1551.

2-(2-(1-Naphthoyl)-8-fluoro-3,4-dihydro-1H-pyrido[4,3-b]indol-5(2H)-yl)acetic Acid (28). Saponification of **10b₁** provided pure **28** after recrystallization from acetonitrile as a beige solid in 93% yield, mp 224.0 °C. LC(1)/ESI-MS t_{R} = 0.83 min; m/z [$\text{M} + \text{H}^+$] = 403.09. ^1H NMR (DMSO- d_6), 65:35 mixture of two rotamers, δ : 8.02 (m, 2 H), 7.76 (d, $J = 7.8$ Hz, 0.65 H), 7.72 (m, 0.35 H), 7.49–7.64 (m, 3.35 H), 7.35–7.49 (m, 2.35 H), 6.98 (ddd, $J_{\text{H-F}} = 9.3$ Hz, $J_1 = 9.3$ Hz, $J_2 = 2.4$ Hz, 0.65 H), 6.88 (m, 0.65 H), 4.85–5.14 (m, 3.3 H), 4.42 (m, 0.35 H), 4.32 (m, 0.7 H), 4.06 (m, 0.35 H), 3.50 (t, $J = 5.5$ Hz, 1.3 H), 2.95 (m, 0.70 H), 2.68 (m, 0.65 H), 2.58 (m, 0.65 H). ^{13}C NMR (DMSO- d_6) δ : 170.7, 169.2, 157.7 (d, $J_{\text{C-F}} = 232$ Hz), 157.4 (d, $J_{\text{C-F}} = 233$ Hz), 137.1, 136.2, 135.1, 134.9, 134.0, 133.8, 133.5, 129.6, 129.5, 129.4, 129.3, 128.9, 128.8, 127.5, 127.4, 127.0, 126.9, 126.0, 125.9, 125.7 (d, $J_{\text{C-F}} = 10$ Hz), 125.2, 125.1, 125.0, 124.1, 123.9, 110.9 (d, $J_{\text{C-F}} = 10$ Hz), 110.8 (m), 109.3 (d, $J_{\text{C-F}} = 26$ Hz), 109.1 (d, $J_{\text{C-F}} = 26$ Hz), 106.7 (m), 103.3 (d, $J_{\text{C-F}} = 23$ Hz), 103.0 (d, $J_{\text{C-F}} = 23$ Hz),

44.73, 44.70, 44.5, 44.4, 39.5, 39.3, 23.1, 22.3. HRMS (ESI): m/z calcd for $\text{C}_{24}\text{H}_{20}\text{N}_2\text{O}_3\text{F}$ [$\text{M} + \text{H}^+$] 403.1458, found 403.1458.

2-(2-(2-(1H-Indol-3-yl)acetyl)-8-fluoro-3,4-dihydro-1H-pyrido[4,3-b]indol-5(2H)-yl)acetic Acid (33). Saponification of **10b₆** provided pure **33** after preparative HPLC as a beige foam in 88% yield. LC(1)/ESI-MS t_{R} = 0.79 min; m/z [$\text{M} + \text{H}^+$] = 406.11. ^1H NMR (DMSO- d_6), 60:40 mixture of two rotamers, δ : 12.75 (m, 1 H), 10.92 (s, 0.6 H), 10.86 (s, 0.4 H), 7.61 (m, 1 H), 7.32–7.44 (m, 2 H), 7.24–7.32 (m, 2 H), 7.07 (m, 1 H), 6.95 (m, 2 H), 4.92 (s, 0.8 H), 4.90 (s, 1.2 H), 4.80 (s, 0.8 H), 4.65 (s, 1.2 H), 3.88 (m, 4 H), 2.69 (d, $J = 5.1$ Hz, 2 H). ^{13}C NMR (DMSO- d_6) δ : 170.8, 170.4, 170.3, 157.5 (d, $J_{\text{C-F}} = 232$ Hz), 157.5 (d, $J_{\text{C-F}} = 231$ Hz), 137.0, 136.6, 136.5, 136.4, 133.9, 133.8, 127.8, 127.7, 125.7 (d, $J_{\text{C-F}} = 10$ Hz), 125.4 (d, $J_{\text{C-F}} = 10$ Hz), 124.0, 123.9, 121.5, 121.4, 119.3, 119.2, 118.9, 118.8, 111.8, 111.7, 110.8, 110.7, 109.0 (d, $J_{\text{C-F}} = 26$ Hz), 108.7, 108.6, 107.1 (d, $J_{\text{C-F}} = 4$ Hz), 107.0 (d, $J_{\text{C-F}} = 4$ Hz), 103.2 (d, $J_{\text{C-F}} = 24$ Hz), 103.1 (d, $J_{\text{C-F}} = 24$ Hz), 44.7, 43.4, 43.0, 39.1, 31.6, 31.5, 23.0, 22.1. HRMS (ESI): m/z calcd for $\text{C}_{23}\text{H}_{21}\text{N}_3\text{O}_3\text{F}$ [$\text{M} + \text{H}^+$] 406.1567, found 406.1564.

2-(2-(4'-Ethyl-[1,1'-biphenyl]-4-carbonyl)-3,4-dihydro-1H-pyrido[4,3-b]indol-5(2H)-yl)acetic Acid (35). Saponification of **10a₄** provided pure **35** after precipitation from acetonitrile as a beige foam in 79% yield. LC(1)/ESI-MS t_{R} = 0.94 min; m/z [$\text{M} + \text{H}^+$] = 439.00. ^1H NMR (DMSO- d_6), 60:40 mixture of two rotamers, δ : 13.06 (m, 1 H), 7.76 (d, $J = 7.9$ Hz, 2 H), 7.64 (d, $J = 8.1$ Hz, 2 H), 7.55 (m, 2.5 H), 7.21–7.48 (m, 3.5 H), 6.83–7.20 (m, 2 H), 4.95 (bs, 2 H), 4.80 (bs, 1.2 H), 4.73 (bs, 0.8 H), 4.05 (bs, 0.8 H), 3.75 (bs, 1.2 H), 2.85 (bs, 2 H), 2.67 (q, $J = 7.5$ Hz, 2 H), 1.23 (t, $J = 7.6$ Hz, 3 H). ^{13}C NMR (DMSO- d_6) δ : 170.9, 170.2 (bs), 144.1, 141.8, 137.2 (m), 135.4 (m), 134.3 (m), 129.0, 128.3–127.9 (m), 127.2, 127.0 (bs), 125.4 (bs), 121.5 (bs), 119.6 (bs), 117.7–118.0 (m), 109.9, 106.4 (bs), 45.2 (m, 2 C atoms), 44.6, 28.3, 23.0 (bs), 22.0 (bs), 16.0. HRMS (ESI): m/z calcd for $\text{C}_{28}\text{H}_{27}\text{N}_2\text{O}_3$ [$\text{M} + \text{H}^+$] 439.2021, found 439.2021.

Solubility Measurements. For each compound 40 μL of 10 mM DMSO stock solution was dispensed into a Millipore MSHVN4510 Multiscreen 96-well filter plate for solubility by means of a BIOMEK NX^P (Beckman Coulter) laboratory automated workstation. The solvents were evaporated under reduced pressure in a Hettich AG Combidancer. Each well was filled with 200 μL of water, 60 mM citrate buffer, pH4, or 70 mM phosphate buffer, pH7. The mixture was stirred on an Eppendorf Thermomixer 5355 comfort at 300 rpm at 25 °C for 24 h. The resulting biphasic system was filtered under reduced pressure using a Millipore MAVM0960R vacuum manifold. The filtrates were collected into a 96-well Thermo Scientific AB0600PCR plate. Solubility was determined by measuring the concentration of the solutions using a high pressure mixing Shimadzu modular HPLC system with a Phenomenex column Synergi Polar-RP 4 μm , 80 \AA , 2.0 cm \times 50 mm warmed at 50 °C: eluent A, water containing 0.05% formic acid; eluent B, acetonitrile containing 0.05% formic acid; gradient, 5–100% A nonlinear gradient over 2.4 min; flow rate of 1.5 mL/min; injection volume, 5 μL . UV detection occurred at 250 nm. Concentrations were determined by comparison of the peak area with the calibration curve.

hCRTh2 Radioligand Binding Assay. The CRTh2 binding assay was established based on previous reports.^{38–40} Membranes of HEK293 cells with recombinant expression of the human CRTH2 receptor were generated. Cells were detached from culture plates in 5 mL of buffer A (5 mM Tris, 1 mM MgCl₂, 0.1 mM PMSF, 0.1 mM phenanthroline, pH 7.4) per plate using a rubber policeman, transferred into centrifugation tubes, and frozen at –80 °C. After thawing, the cells were fragmented by homogenization with a Polytron cell homogenizer for 30 s. The membrane fragments were collected by centrifugation at 30000g for 20 min and resuspended in buffer B (75 mM Tris, 25 mM MgCl₂, 250 mM saccharose, pH 7.4). Aliquots were stored at –20 °C.

The binding assay was performed in a final assay volume of 250 μL . In each well, an amount of 75 μL of buffer C (50 mM Tris, pH 7.4, 100 mM NaCl, 1 mM EDTA, 0.1% protease free BSA, 0.01% NaN₃) was mixed with 50 μL of [³H]PGD₂ (2.5 nM, 220 000 dpm/well, Amersham Biosciences, TRK734) and 25 μL of a solution of test

compound in buffer C containing 10% DMSO. The binding assay was started by adding 100 μL of a membrane suspension in buffer C, reaching a final concentration of 80 μg of membrane protein per well. Nonspecific binding was determined in the presence of 10 μM PGD₂. This binding assay mix was incubated at room temperature for 90 min and then filtered through a GF/C filter 96-well plate which was presoaked in 0.5% PEI for 3 h. The filter wells were washed three times with ice cold binding buffer C. Then Microscint-40 (Packard, 40 μL per well) was added and the receptor bound radioactivity was quantified by scintillation counting in a "TopCount" benchtop microplate scintillation counter (Packard).

hCRTh2 Intracellular Calcium Liberation (FLIPR) Assay. Human embryonic kidney cells (HEK-293, DSMZ) stably expressing the human CRTh2 receptor under the control of the CMV promoter were grown to near confluency in DMEM medium (1 g/L glucose, Gibco) supplemented with 10% fetal calf serum (Pan) containing penicillin and streptomycin (100 units/mL each, Gibco) under standard mammalian cell culture conditions at 37 °C in a humidified atmosphere of 5% CO₂. Cells were detached from culture dishes with a cell dissociation buffer (0.02% EDTA in PBS, Gibco) for 1 min, washed off with DMEM without phenol red (Gibco), and collected by centrifugation with 200g at room temperature for 5 min. The cells were incubated with 4 μM Fluo-4 AM ester (Teflabs) in DMEM (without phenol red) in 20 mM HEPES, pH 7.2 (Gibco), at 37 °C in a humidified atmosphere of 5% CO₂ for 40 min. Then they were washed with and resuspended in assay buffer (HBSS with 20 mM HEPES, pH 7.2). Resuspended cells, 100 000 in 60 μL per well, were seeded onto a 384-well clear-bottom black assay plate (Greiner), sedimented by centrifugation, and incubated at room temperature for 15 min. Stock solutions of test compounds were made up at a concentration of 10 mM in DMSO and serially diluted in assay buffer to concentrations required for dose–response curves. PGD₂ (Biomol, Plymouth Meeting, PA) is used as an agonist. A FLIPRII instrument (Molecular Devices) was operated following the manufacturer's instructions. Test compound (10 μL) was added to each well and incubated for 5 min. Cells were activated by a final concentration of 50 nM PGD₂ (Biomol, Plymouth Meeting, PA) dissolved in the assay buffer supplemented with 0.05% bovine serum albumin (fatty acid content of <0.02%, Sigma). Fluorescence emission was recorded during test compound and PGD₂ addition, and emission peak values above base level after PGD₂ addition were exported. Values were normalized to high-level control (no antagonist added) after subtraction of baseline value control (no PGD₂ added). The IC₅₀ values were calculated by four-parameter dose–response curve fitting (XLfit, ISBS).

Intracellular cAMP Assay. Cells were cultured in 96-well plates to reach about 80% confluency (10 000 cells seeded 3 days before experiment) using the same growth conditions as described above. The culture medium was removed and the stimulation started by addition of 100 μL /well DMEM containing 50 μM IBMX (3-isobutyl-1-methylxanthine), various concentrations of test compound, 100 nM PGD₂, and 10 μM forskolin. After a 20 min incubation time at 37 °C intracellular cAMP concentrations were quantified using the Tropix cAMP-screen chemiluminescent ELISA system (Applied Biosystems) following the instructions provided in the kit. Briefly, cells were solubilized by addition of 100 μL of lysis buffer (provided in assay kit) and incubated for 30 min at 37 °C. Then an amount of 60 μL per well of the cAMP–alkaline phosphatase conjugate, diluted 1:100, followed by 60 μL of anti-cAMP antibody was added. After 1 h of incubation, the solution was removed and washed six times with washing buffer. Then 100 μL /well CSPD/Sapphire-II RTU substrate enhancer solution was added and incubated for 30 min. The signal was quantified in the luminometer PHERAstar (BMG Labtech). Absolute cAMP concentrations were then determined using a standard cAMP curve that was generated in parallel.

Shape Change of Human Eosinophils. After healthy volunteers had given informed consent, blood samples were drawn by venipuncture according to the protocol approved by the ethics committee of Basel (Switzerland). Polymorphonuclear leukocytes (containing eosinophils, basophils, and neutrophils) were isolated using the Polymorphprep method according to the manufacturer's

protocol (Axis-Shield). In brief, anticoagulated whole blood was layered onto a Polymorphprep gradient (density, 1.113 g/mL) and centrifuged at 500g for 30 min. The polymorphonuclear fraction was harvested and depleted for erythrocytes by hypotonic saline lysis.

The polymorphonuclears (PMNs) were resuspended in assay buffer composed of PBS with Ca²⁺/Mg²⁺ supplemented with 0.1% BSA, 10 mM Hepes, and 10 mM glucose, pH 7.4, with 10⁶ cells/mL and stained with CD49d-APC (allophycocyanin conjugated mouse anti-human VLA-4) for 1 h at room temperature. Next, 45 μL of human plasma was mixed with 10 μL of assay buffer and 30 μL of PMNs (1.3 \times 10⁷ cells/mL) were mixed. The PMNs were then activated by addition of 15 nM PGD₂ and incubated for 5 min at 37 °C. The activation was stopped by addition of 100 μL of ice cold 1% paraformaldehyde. The samples were analyzed with a FACSaria flow cytometer (BD Biosciences). Eosinophils were identified based on the fluorescence signal (CD49d-APC (Allophycocyanin (APC)) and side scatter (SSC). The data recorded in our experiments were gated to detect the eosinophil cell population only. Eosinophil activation was quantified based on increase in forward scatter (FSC). Activation was expressed as the percent of cells with a forward scatter larger than that of nonactivated eosinophils.

■ ASSOCIATED CONTENT

📄 Supporting Information

Detailed experimental procedures and analytical data (Tables S1–S5) of synthesized compounds 11–21, 23, 25, 27, 29–32, 34, 36 and the respective precursors; method for the determination of the log *D* values; experimental details for the biological assays used to assess the receptor selectivity, for the cytochrome P450 enzyme inhibition assays, and for the metabolic stability studies; and the detailed description of the pharmacokinetic studies in the rat and the dog. This material is available free of charge via the Internet at <http://pubs.acs.org>.

■ AUTHOR INFORMATION

✉ Corresponding Author

*Phone: +41-61-565-6208. E-mail: heinz.fretz@actelion.com.

Author Contributions

The manuscript was written through contributions of all authors. All authors have given approval to the final version of the manuscript.

Notes

The authors declare no competing financial interest.

■ ACKNOWLEDGMENTS

The authors thank S. Koch, D. Lotz, A. Jonuzi, P. Risch, B. Butscha, J. Giller, B. Lack, M. Baumann, and S. Brand for technical support; B. Capeleto for physicochemical and Francois Le Goff for stability measurements in different solution media; R. Bravo for formulation work; S. Delahaye and H. Kletzl for providing DMPK data; M. Holdener for supportive discussions; and J. Williams for proofreading the manuscript.

■ ABBREVIATIONS USED

APC, allophycocyanin; Boc₂O, di-*tert*-butyl dicarbonate; bs, broad singlet; CHO, chinese hamster ovary; Cl, clearance; Cl_{int}, intrinsic clearance; CRTh2, chemoattractant receptor-homologous molecule expressed on Th2 cells; Da, dalton; DAD, diode-array detector; DIPEA, diisopropylethylamine; DMEM, Dulbecco's modified Eagle medium; ELSD, evaporative light scattering detector; EtOAc, ethyl acetate; FCS, fetal calf serum; f_{HSA}, shift factor in human serum albumin; FLIPR, fluorometric imaging plate reader; FSC, forward scatter; f_{sel}, selectivity

factor; HBSS, Hank's balanced salt solution; *hDP*₁, human prostaglandin D₂ receptor subtype 1; *hEP*₁, human prostaglandin E₂ receptor subtype 1; *hEP*₂, human prostaglandin E₂ receptor subtype 2; *hEP*₃, human prostaglandin E₂ receptor subtype 3; *hEP*₄, human prostaglandin E₂ receptor subtype 4; HEPES, 4-(2-hydroxyethyl)-1-piperazineethanesulfonic acid; *hESC*, human eosinophil shape change assay; HLM, human liver microsomes; HSA, human serum albumin; *hTP*, human thromboxane A₂ receptor; HTRF, homogeneous time-resolved fluorescence; IBMX, 3-isobutyl-1-methylxanthine; IL, interleukin; LE, ligand efficiency; log *D*_{7.4}, measured log *D* at pH 7.4; mmol, millimole; PDA, photodiode array; PEI, polyethyleneimine; PG, propylene glycol; PGD₂, prostaglandin D₂; PGDS, prostaglandin synthase; PMSF, phenylmethanesulfonyl fluoride; PMN, polymorphonuclear; RHepa, rat hepatocyte; RLM, rat liver microsome; SGF, simulated gastric fluid; SIF, simulated intestinal fluid; SSC, side scatter; Th2, T-helper 2; TL, traffic light; TXA₂, thromboxane A₂; *V*_{ss}, volume of distribution at steady state

REFERENCES

- (1) Papadopoulos, N. G.; Agache, I.; Bavbek, S.; Bilo, B. M.; Braidó, F.; Cardona, V.; Custovic, A.; Demonchy, J.; Demoly, P.; Eigenmann, P.; Gayraud, J.; Grattan, C.; Heffler, E.; Hellings, P. W.; Jutel, M.; Knol, E.; Lotvall, J.; Muraro, A.; Poulsen, L. K.; Roberts, G.; Schmid-Grendelmeier, P.; Skevaki, C.; Triggiani, M.; Vanree, R.; Werfel, T.; Flood, B.; Palkonen, S.; Savli, R.; Allegri, P.; Annesi-Maesano, I.; Annunziato, F.; Antolin-Amerigo, D.; Apfelbacher, C.; Blanca, M.; Bogacka, E.; Bonadonna, P.; Bonini, M.; Boyman, O.; Brockow, K.; Burney, P.; Buters, J.; Butiene, I.; Calderon, M.; Cardell, L. O.; Caubet, J. C.; Celenk, S.; Cichočka-Jarosz, E.; Cingi, C.; Couto, M.; Dejong, N.; Del Giacco, S.; Douladiris, N.; Fassio, F.; Fauquet, J. L.; Fernandez, J.; Rivas, M. F.; Ferrer, M.; Flohr, C.; Gardner, J.; Genuneit, J.; Gevaert, P.; Groblewska, A.; Hamelmann, E.; Hoffmann, H. J.; Hoffmann-Sommergruber, K.; Hovhannisyan, L.; Hox, V.; Jahnsen, F. L.; Kalayci, O.; Kalpaklioglu, A. F.; Kleine-Tebbe, J.; Konstantinou, G.; Kurowski, M.; Lau, S.; Lauener, R.; Lauerma, A.; Logan, K.; Magnan, A.; Makowska, J.; Makrinioti, H.; Mangina, P.; Manole, F.; Mari, A.; Mazon, A.; Mills, C.; Mingomataj, E.; Niggemann, B.; Nilsson, G.; Ollert, M.; O'Mahony, L.; O'Neil, S.; Pala, G.; Papi, A.; Passalacqua, G.; Perkin, M.; Pfaar, O.; Pitsios, C.; Quirce, S.; Raap, U.; Raulf-Heimsoth, M.; Rhyner, C.; Robson-Ansley, P.; Alves, R. R.; Roje, Z.; Rondon, C.; Rudzvieciene, O.; Rueff, F.; Rukhadze, M.; Rumi, G.; Sackesen, C.; Santos, A. F.; Santucci, A.; Scharf, C.; Schmidt-Weber, C.; Schnyder, B.; Schwarze, J.; Senna, G.; Sergejeva, S.; Seys, S.; Siracusa, A.; Skypala, I.; Sokolowska, M.; Spertini, F.; Spiwak, R.; Sprickelmann, A.; Sturm, G.; Swoboda, I.; Terreehorst, I.; Toskala, E.; Traidl-Hoffmann, C.; Venter, C.; Vlieg-Boerstra, B.; Whitacker, P.; Worm, M.; Xepapadaki, P.; Akdis, C. A. Research needs in allergy: an EAACI position paper, in collaboration with EFA. *Clin. Transl. Allergy* **2012**, *2* (21), 1–23.
- (2) Barnes, P. J. New drugs for asthma. *Semin. Respir. Crit. Care Med.* **2012**, *33*, 685–694.
- (3) Quirce, S.; Bobolea, I.; Barranco, P. Emerging drugs for asthma. *Expert. Opin. Emerging Drugs* **2012**, *17*, 219–237.
- (4) Peters, S. P.; Schleimer, R. P.; Kagey-Sobotka, A.; Naclerio, R. M.; MacGlashan, D. W., Jr.; Schulman, E. S.; Adkinson, N. F., Jr.; Lichtenstein, L. M. The role of prostaglandin D₂ in IgE-mediated reactions in man. *Trans. Assoc. Am. Physicians* **1982**, *95*, 221–228.
- (5) Lewis, R. A.; Soter, N. A.; Diamond, P. T.; Austen, K. F.; Oates, J. A.; Roberts, L. J., 2nd. Prostaglandin D₂ generation after activation of rat and human mast cells with anti-IgE. *J. Immunol.* **1982**, *129*, 1627–1631.
- (6) Crea, A. E.; Nakhosteen, J. A.; Lee, T. H. Mediator concentrations in bronchoalveolar lavage fluid of patients with mild asymptomatic bronchial asthma. *Eur. Respir. J.* **1992**, *5*, 190–195.
- (7) Liu, M. C.; Bleecker, E. R.; Lichtenstein, L. M.; Kagey-Sobotka, A.; Niv, Y.; McLemore, T. L.; Permutt, S.; Proud, D.; Hubbard, W. C. Evidence for elevated levels of histamine, prostaglandin D₂, and other bronchoconstricting prostaglandins in the airways of subjects with mild asthma. *Am. Rev. Respir. Dis.* **1990**, *142*, 126–132.
- (8) Hirai, H.; Tanaka, K.; Yoshie, O.; Ogawa, K.; Kenmotsu, K.; Takamori, Y.; Ichimasa, M.; Sugamura, K.; Nakamura, M.; Takano, S.; Nagata, K. Prostaglandin D₂ selectively induces chemotaxis in T helper type 2 cells, eosinophils, and basophils via seven-transmembrane receptor CRTH2. *J. Exp. Med.* **2001**, *193*, 255–261.
- (9) Mjosberg, J. M.; Trifari, S.; Crellin, N. K.; Peters, C. P.; van Drunen, C. M.; Piet, B.; Fokkens, W. J.; Cupedo, T.; Spits, H. Human IL-25- and IL-33-responsive type 2 innate lymphoid cells are defined by expression of CRTH2 and CD161. *Nat. Immunol.* **2011**, *12*, 1055–1062.
- (10) Xue, L.; Gyles, S. L.; Wettestad, F. R.; Gazi, L.; Townsend, E.; Hunter, M. G.; Pettipher, R. Prostaglandin D₂ causes preferential induction of proinflammatory Th2 cytokine production through an action on chemoattractant receptor-like molecule expressed on Th2 cells. *J. Immunol.* **2005**, *175*, 6531–6536.
- (11) Yoshimura-Uchiyama, C.; Iikura, M.; Yamaguchi, M.; Nagase, H.; Ishii, A.; Matsushima, K.; Yamamoto, K.; Shichijo, M.; Bacon, K. B.; Hirai, K. Differential modulation of human basophil functions through prostaglandin D₂ receptors DP and chemoattractant receptor-homologous molecule expressed on Th2 cells/DP2. *Clin. Exp. Allergy* **2004**, *34*, 1283–1290.
- (12) Tanaka, K.; Hirai, H.; Takano, S.; Nakamura, M.; Nagata, K. Effects of prostaglandin D₂ on helper T cell functions. *Biochem. Biophys. Res. Commun.* **2004**, *316*, 1009–1014.
- (13) Wills-Karp, M.; Luyimbazi, J.; Xu, X.; Schofield, B.; Neben, T. Y.; Karp, C. L.; Donaldson, D. D. Interleukin-13: central mediator of allergic asthma. *Science* **1998**, *282*, 2258–2261.
- (14) Grunig, G.; Warnock, M.; Wakil, A. E.; Venkayya, R.; Brombacher, F.; Rennick, D. M.; Sheppard, D.; Mohrs, M.; Donaldson, D. D.; Locksley, R. M.; Corry, D. B. Requirement for IL-13 independently of IL-4 in experimental asthma. *Science* **1998**, *282*, 2261–2263.
- (15) Matsuoka, T.; Hirata, M.; Tanaka, H.; Takahashi, Y.; Murata, T.; Kabashima, K.; Sugimoto, Y.; Kobayashi, T.; Ushikubi, F.; Aze, Y.; Eguchi, N.; Urade, Y.; Yoshida, N.; Kimura, K.; Mizoguchi, A.; Honda, Y.; Nagai, H.; Narumiya, S. Prostaglandin D₂ as a mediator of allergic asthma. *Science* **2000**, *287*, 2013–2017.
- (16) Kostenis, E.; Ulven, T. Emerging roles of DP and CRTH2 in allergic inflammation. *Trends Mol. Med.* **2006**, *12*, 148–158.
- (17) Hart, F. D.; Boardman, P. L. Indomethacin: a new non-steroid anti-inflammatory agent. *Br. Med. J.* **1963**, *2*, 965–970.
- (18) Hirai, H.; Tanaka, K.; Takano, S.; Ichimasa, M.; Nakamura, M.; Nagata, K. Cutting edge: agonistic effect of indomethacin on a prostaglandin D₂ receptor, CRTH2. *J. Immunol.* **2002**, *168*, 981–985.
- (19) Rosentreter, U.; Boshagen, H.; Seuter, F.; Perzborn, E.; Fiedler, V. B. Synthesis and absolute configuration of the new thromboxane antagonist (3R)-3-(4-fluorophenylsulfonamido)-1,2,3,4-tetrahydro-9-carbazolepropanoic acid and comparison with its enantiomer. *Arzneim. Forsch.* **1989**, *39*, 1519–1521.
- (20) Aizawa, H.; Shigyo, M.; Nogami, H.; Hirose, T.; Hara, N. BAY u3405, a thromboxane A₂ antagonist, reduces bronchial hyper-responsiveness in asthmatics. *Chest* **1996**, *109*, 338–342.
- (21) Terada, N.; Yamakoshi, T.; Hasegawa, M.; Tanikawa, H.; Maesako, K.; Ishikawa, K.; Konno, A. The effect of ramatroban (BAY u 3405), a thromboxane A₂ receptor antagonist, on nasal cavity volume and minimum cross-sectional area and nasal mucosal hemodynamics after nasal mucosal allergen challenge in patients with perennial allergic rhinitis. *Acta Otolaryngol. Suppl.* **1998**, *537*, 32–37.
- (22) Sugimoto, H.; Shichijo, M.; Iino, T.; Manabe, Y.; Watanabe, A.; Shimazaki, M.; Gantner, F.; Bacon, K. B. An orally bioavailable small molecule antagonist of CRTH2, ramatroban (BAY u3405), inhibits prostaglandin D₂-induced eosinophil migration in vitro. *J. Pharmacol. Exp. Ther.* **2003**, *305*, 347–352.

(23) Pettipher, R.; Whittaker, M. Update on the development of antagonists of chemoattractant receptor-homologous molecule expressed on Th2 cells (CRTH2). From lead optimization to clinical proof-of-concept in asthma and allergic rhinitis. *J. Med. Chem.* **2012**, *55*, 2915–2931.

(24) Valdenaire, A.; Pothier, J.; Renneberg, D.; Riederer, M. A.; Peter, O.; Leroy, X.; Gnerre, C.; Fretz, H. Evolution of novel tricyclic CRTH2 receptor antagonists from a (*E*)-2-cyano-3-(1*H*-indol-3-yl)acrylamide scaffold. *Bioorg. Med. Chem. Lett.* **2013**, *23*, 944–948.

(25) Boie, Y.; Sawyer, N.; Slipetz, D. M.; Metters, K. M.; Abramovitz, M. Molecular cloning and characterization of the human prostanoid DP receptor. *J. Biol. Chem.* **1995**, *270*, 18910–18916.

(26) Stubbs, V. E.; Schratl, P.; Hartnell, A.; Williams, T. J.; Peskar, B. A.; Heinemann, A.; Sabroe, I. Indomethacin causes prostaglandin D(2)-like and eotaxin-like selective responses in eosinophils and basophils. *J. Biol. Chem.* **2002**, *277*, 26012–26020.

(27) Sabroe, I.; Hartnell, A.; Jopling, L. A.; Bel, S.; Ponath, P. D.; Pease, J. E.; Collins, P. D.; Williams, T. J. Differential regulation of eosinophil chemokine signaling via CCR3 and non-CCR3 pathways. *J. Immunol.* **1999**, *162*, 2946–2955.

(28) Fretz, H.; Fecher, A.; Hilpert, K.; Riederer, M. A. Preparation of Tetrahydropyridoindole Derivatives as CRTH2 Receptor Antagonists for the Treatment of Prostaglandin-Mediated Diseases PCT Int. Appl. WO 2005095397 A1 20051013, 2005.

(29) Hopkins, A. L.; Groom, C. R.; Alex, A. Ligand efficiency: a useful metric for lead selection. *Drug Discovery Today* **2004**, *9*, 430–431.

(30) Lipinski, C. A. Drug-like properties and the causes of poor solubility and poor permeability. *J. Pharmacol. Toxicol. Methods* **2000**, *44*, 235–249.

(31) Asafu-Adjaye, E. B.; Faustino, P. J.; Tawakkul, M. A.; Anderson, L. W.; Yu, L. X.; Kwon, H.; Volpe, D. A. Validation and application of a stability-indicating HPLC method for the in vitro determination of gastric and intestinal stability of venlafaxine. *J. Pharm. Biomed. Anal.* **2007**, *43*, 1854–1859.

(32) Lobell, M.; Hendrix, M.; Hinzen, B.; Keldenich, J.; Meier, H.; Schmeck, C.; Schohe-Loop, R.; Wunberg, T.; Hillisch, A. In silico ADMET traffic lights as a tool for the prioritization of HTS hits. *ChemMedChem* **2006**, *1*, 1229–1236.

(33) Tanimoto, N.; Hiramatsu, Y.; Mitsumori, S.; Inagaki, M., Preparation of Indole Derivatives as PGD2 Receptor Antagonists. PCT Int. Appl. WO 2003097598 A1 20031127, 2003.

(34) Ruediger, E. H.; Deon D., H.; Kadow, J. F. Preparation of Tetrahydrocarbolines for Treatment of HIV Infection and AIDS. U.S. Pat. Appl. Publ. US 20050267130 A1 20051201, 2005.

(35) Bonjoch, J.; Diaba, F.; Pages, L.; Perez, D.; Soca, L.; Miralpeix, M.; Vilella, D.; Anton, P.; Puig, C. Synthesis and structure–activity relationships of gamma-carboline derivatives as potent and selective cysLT(1) antagonists. *Bioorg. Med. Chem. Lett.* **2009**, *19*, 4299–4302.

(36) Ivashchenko, A. A.; Ivashchenko, A. V.; Tkachenko, S. Y.; Okun, I. M.; Savchuk, N. F.; Mitkin, O. D.; Kravchenko, V. Substituted 2,3,4,5-Tetrahydro-1*H*-pyrido[4,3-*b*]indoles as Novel Antihistaminic Agents and Processes for Preparation Thereof. PCT Int. Appl. WO 2008115098 A2 20080925, 2008.

(37) Ivashchenko, A. V.; Mit'kin, O. D.; Kisil, V. M.; Frolov, E. B.; Tkachenko, S. E. *Izv. Vyssh. Uchebn. Zaved., Khim. Khim. Tekhnol.* **2009**, *52*, 78–83.

(38) Shimizu, T.; Yamashita, A.; Hayaishi, O. Specific binding of prostaglandin D2 to rat brain synaptic membrane. Occurrence, properties, and distribution. *J. Biol. Chem.* **1982**, *257*, 13570–13575.

(39) Fortini, A.; Modesti, P. A.; Abbate, R.; Gensini, G. F.; Neri Serneri, G. G. Heparin does not interfere with prostacyclin and prostaglandin D2 binding to platelets. *Thromb. Res.* **1985**, *40*, 319–328.

(40) Sawyer, N.; Cauchon, E.; Chateaufneuf, A.; Cruz, R. P.; Nicholson, D. W.; Metters, K. M.; O'Neill, G. P.; Gervais, F. G. Molecular pharmacology of the human prostaglandin D2 receptor, CRTH2. *Br. J. Pharmacol.* **2002**, *137*, 1163–1172.